

**Aerosol effects on
deep convection**

Z. J. Lebo and
J. H. Seinfeld

This discussion paper is/has been under review for the journal Atmospheric Chemistry and Physics (ACP). Please refer to the corresponding final paper in ACP if available.

Theoretical basis for convective invigoration due to increased aerosol concentration

Z. J. Lebo¹ and J. H. Seinfeld^{1,2}

¹Environmental Science and Engineering, California Institute of Technology, Pasadena, 91125, CA, USA

²Chemical Engineering, California Institute of Technology, Pasadena, 91125, CA, USA

Received: 3 January 2011 – Accepted: 8 January 2011 – Published: 24 January 2011

Correspondence to: Z. J. Lebo (zachlebo@caltech.edu)

Published by Copernicus Publications on behalf of the European Geosciences Union.

Title Page

Abstract

Introduction

Conclusions

References

Tables

Figures

⏪

⏩

◀

▶

Back

Close

Full Screen / Esc

Printer-friendly Version

Interactive Discussion



Abstract

The potential effects of increased aerosol loading on the development of deep convective clouds and resulting precipitation amounts are studied by employing the Weather Research and Forecasting (WRF) model as a detailed high-resolution cloud resolving model (CRM) with both detailed bulk and bin microphysics schemes. The bulk microphysics scheme incorporates a physically based parameterization of cloud droplet activation as well as homogeneous and heterogeneous freezing in order to explicitly resolve the possible aerosol-induced effects on the cloud microphysics. These parameterizations allow one to segregate the effects of an increase in the aerosol number concentration into enhanced cloud condensation nuclei (CCN) and/or ice nuclei (IN) concentrations using bulk microphysics. The bin microphysics scheme, with its explicit calculations of cloud particle collisions, is shown to better predict cumulative precipitation. Increases in the CCN number concentration may not have a monotonic influence on the cumulative precipitation resulting from deep convective clouds. We demonstrate that the aerosol-induced effect is controlled by the balance between latent heating and the increase in condensed water aloft, each having opposing effects on buoyancy. It is also shown that under polluted conditions and in relatively dry environments, increases in the CCN number concentration reduce the cumulative precipitation due to the competition between the sedimentation and evaporation/sublimation timescales. The effect of an increase in the IN number concentration on the dynamics of deep convective clouds is small, but may act to suppress precipitation.

A comparison of the predictions using the bin and bulk microphysics schemes demonstrate a significant difference between the predicted precipitation and the influence of aerosol perturbations on updraft velocity within the convective core. The bulk microphysics scheme is shown to be unable to capture the changes in latent heating that occur as a result of changes in the CCN number concentration, while the bin microphysics scheme demonstrates significant increases in the latent heating aloft with increasing CCN number concentration. This suggests that a detailed two-bulk

ACPD

11, 2773–2842, 2011

Aerosol effects on deep convection

Z. J. Lebo and
J. H. Seinfeld

Title Page

Abstract

Introduction

Conclusions

References

Tables

Figures

◀

▶

◀

▶

Back

Close

Full Screen / Esc

Printer-friendly Version

Interactive Discussion



microphysics scheme, which is more computationally efficient than bin microphysics schemes, may not be sufficient, even when coupled to a detailed activation scheme, to predict small changes that result from perturbations in aerosol loading.

1 Introduction

5 Changes in ambient concentrations of cloud condensation nuclei (CCN) and ice nuclei (IN) potentially alter cloud properties that may ultimately lead to modifications in cloud radiative forcing and/or precipitation. Traditionally, aerosol-cloud interactions have been discussed primarily in terms of (IPCC, 2007): (1) The “1st aerosol indirect effect” (Twomey, 1977), in which all else being equal, an increase in the CCN
10 number concentration will result in a higher cloud droplet number concentration and hence smaller particles. More numerous smaller particles act to increase the cloud optical depth and thus the cloud albedo that ultimately results in a reduction of the shortwave radiative flux that reaches the surface (cooling effect at the surface). (2) The “2nd aerosol indirect effect” (Albrecht, 1989), in which changes in the CCN number
15 concentration may affect cloud lifetime and precipitation efficiency. An increase in the CCN number concentration will result in smaller cloud droplets, for which the collection kernels and collection efficiencies are substantially smaller in comparison to their larger counterparts, thus mitigating the collision-coalescence process and suppressing precipitation. Ultimately, the additional CCN particles are hypothesized to increase the
20 longevity of the cloud and reduce the surface heating by shortwave radiation (cooling effect at the surface). With that said, it is now recognized that a division into the 1st and 2nd indirect effects is an oversimplification of the continuous cascade of processes that ensue in response to a perturbation in the aerosol number concentration.

25 Considerable attention has been given to the effects of aerosol particles on cloud properties for warm stratiform clouds (e.g., Ackerman et al., 2004; Lu and Seinfeld, 2006; Sandu et al., 2008; Hill et al., 2008, 2009; Wang and Feingold, 2009a,b; Wang et al., 2010). The extent to which these processes hold in mixed-phase and/or cold

Aerosol effects on deep convection

Z. J. Lebo and
J. H. Seinfeld

Title Page

Abstract

Introduction

Conclusions

References

Tables

Figures

◀

▶

◀

▶

Back

Close

Full Screen / Esc

Printer-friendly Version

Interactive Discussion



clouds is not well established. The ice phase presents significant complexities not present in warm clouds (i.e., riming, aggregation, accretion, heterogeneous and homogeneous freezing, melting, etc.), and the cold-rain process is the predominant mechanism by which rain forms (not collision-coalescence of liquid drops). Recently, the potential effects of polluted environments on the formation and development of deep convective clouds have received attention via both modeling studies (e.g., Koren et al., 2005; Van den Hoever et al., 2006; Van den Hoever and Cotton, 2007; Khain et al., 2008; Rosenfeld et al., 2008a; Stevens and Feingold, 2009; Khain and Lynn, 2009; Fan et al., 2009) and, less commonly, observational analyses (e.g., Koren et al., 2010).

Conceptual hypotheses have been put forth by Rosenfeld et al. (2008a) and Stevens and Feingold (2009) for the invigoration of deep convective clouds by increased aerosol loading. These works are discussed in further detail below. Briefly however, via different reasoning, both works conclude that an increase in aerosol number concentration should act to increase surface precipitation. Although this makes sense conceptually, modeling studies are still not in agreement as to the sign of the effect on precipitation owing to increased pollutants. For example, Van den Hoever et al. (2006) showed that adding aerosol particles in the form of CCN, giant CCN (GCCN), and/or IN causes a decrease in domain-average cumulative precipitation in reference to a clean environment observed during the Cirrus Regional Study of Tropical Anvils and Cirrus Layer-Florida Area Cirrus Experiment (CRYSTAL-FACE). On the other hand, Khain and Lynn (2009) demonstrated an increase in precipitation with an increase in CCN concentration using a spectral bin microphysics model but with low spatial resolution and abbreviated simulation time. In the same study, a decrease in precipitation with an increase in CCN number concentration was shown using a simple two-moment bulk microphysics scheme.

One can imagine though that the effect of an increase in the ambient aerosol concentration on surface precipitation (as well as cloud radiative forcing) in deep convective clouds may not be monotonic and likely depends significantly on the environmental conditions. Khain et al. (2008) attempted to classify the effects of increased aerosol

Aerosol effects on deep convectionJ. Z. Lebo and
J. H. Seinfeld

Title Page

Abstract

Introduction

Conclusions

References

Tables

Figures

◀

▶

◀

▶

Back

Close

Full Screen / Esc

Printer-friendly Version

Interactive Discussion



Aerosol effects on deep convectionZ. J. Lebo and
J. H. Seinfeld

Title Page

Abstract

Introduction

Conclusions

References

Tables

Figures

◀

▶

◀

▶

Back

Close

Full Screen / Esc

Printer-friendly Version

Interactive Discussion



concentrations on precipitation for a wide range of cloud types and locations showing that, for example, deep convective clouds in dry environments should exhibit a decrease in precipitation with an increase in the aerosol number concentration. On the other hand, in moist environments, an increase in the aerosol loading was shown to increase precipitation or provide a negligible change depending on the specific cloud type. Moreover, Fan et al. (2009) showed that in regions with high vertical wind shear, additional aerosol particles are unable to significantly alter the cloud microphysics and thus little change in the surface precipitation is predicted. When the vertical wind shear is reduced, convection is shown to be invigorated due to increased aerosol loading.

Additional studies have looked at the potential implications of aerosol perturbations on the anvil cloud development and microphysical characteristics. The cloud resolving model (CRM) study of Van den Hoever et al. (2006) showed that the anvil clouds atop the simulated deep convective clouds cover less area but contain higher amounts of condensed water when the aerosol number concentration is elevated. This results in more intense, localized precipitation. More recently, satellite data analysis has shown that regions with higher aerosol concentrations statistically correlate with areas of larger cloud extent, i.e., broader anvils (Koren et al., 2010). By broadening the anvil, the cloud becomes thinner and thus reduces the cloud albedo which, in turn, results in an increase in the solar radiation reaching the surface. Little observational evidence is available at this time (due to the inherent complexities in measuring small concentrations of IN in regions of very high instability and remote locations) to determine clearly the overall effect of aerosol perturbations on anvil cloud development.

Measurements of IN number concentration were performed during CRYSTAL-FACE within a period of enhanced dust particle concentration (DeMott et al., 2003; Sassen et al., 2003). DeMott et al. (2003) reported that during CRYSTAL-FACE, IN number concentrations were observed to be as high as 1 cm^{-3} ($10^3 \ell^{-1}$). Later, Van den Hoever et al. (2006) and Teller and Levin (2006) demonstrated a decrease in precipitation with an increase in IN concentration using 3-D and 2-D CRMs, respectively. However, these studies do not fully represent the potential effects of IN on deep convective cloud

development since the freezing process is parameterized based on the empirical relation of Meyers et al. (1992) in which the IN number concentration is expressed as an exponential function of temperature and/or supersaturation. For low temperatures (i.e., less than about -30°C), the IN number concentration, as predicted by the empirical relations, becomes erroneously large and will likely significantly impacts the model predictions.

Microphysical calculations of deep convective cloud invigoration in response to aerosol changes have been performed in recent years (e.g., Khain et al., 2004, 2008; Teller and Levin, 2006; Khain and Lynn, 2009). Potential shortcomings exist in the method by which the CCN concentration is implemented and in the representation of the IN number concentration by the empirical Twomey (1959) relationship to predict the number of activated aerosol particles as a function of supersaturation. The empirical constants in this relation are specific to individual cloud types, i.e., the coefficients that apply for the convective core may not be adequate for other regions of the deep convective cloud, e.g., detrained stratocumulus. Moreover, some of the previous studies have used two-dimensional models (e.g., Khain et al., 2004, 2008; Teller and Levin, 2006) and others that have simulated all three dimensions (e.g., Khain and Lynn, 2009) have been performed at rather low spatial resolution, i.e., ≥ 2 km in the horizontal. It is natural to ask if with limited computational resources, should one simulate deep convective clouds using detailed bin microphysics or instead use a detailed two-moment bulk scheme at much higher spatial resolution? And, if one accounts for the activation of cloud droplets and nucleation of ice particles in a more physically coherent manner, what are the effects of aerosol particles on precipitation in deep convective clouds? These points are addressed in this study.

The remainder of this work is organized as follows: Sect. 2 presents hypotheses regarding aerosol effects on deep convective clouds. This is followed in Sect. 3 by a detailed description of the bulk and bin microphysics models that are employed in this study. Section 4 provides information relevant to the chosen dynamical model as well as details on the model initialization and simulations. Sections 5 and 6 discuss our

Aerosol effects on deep convectionZ. J. Lebo and
J. H. Seinfeld

Title Page

Abstract

Introduction

Conclusions

References

Tables

Figures

◀

▶

◀

▶

Back

Close

Full Screen / Esc

Printer-friendly Version

Interactive Discussion



findings regarding the influence of CCN and IN on deep convective clouds, respectively, and include a detailed comparison of the simulations performed with both the bulk and bin microphysics schemes. Lastly, Sect. 7 concludes the work and serves to outline the most important findings of this study.

2 Theoretical basis and hypotheses

Here, we highlight and discuss recent work in the realm of aerosol invigoration of deep convective cloud. Our purpose here is to present the relevant hypotheses related to this work in a concise framework.

2.1 Rosenfeld et al. (2008a)

Rosenfeld et al. (2008a) argue that the effect of an increased concentration of sub-cloud aerosol, and hence cloud condensation nuclei (CCN), on convective clouds is to invigorate updrafts and produce an increase in precipitation as a result of upward heat transport via phase change. The argument is based on the results of a bulk thermodynamic parcel model, in which in the baseline simulation it is assumed that all water condenses and is immediately precipitated; hence, no energy is required to lift the hydrometeors (for the purpose of this study, hydrometeors are defined to be liquid cloud drops, pristine ice crystals, dendritic snow crystals, and rimed ice, or graupel). In other words, the work required, here in the form of mechanical energy, to lift condensed forms of water is zero. It is assumed, in addition, that the liquid water freezes at -4°C such that when the hydrometeors freeze at and above the level where this temperature is attained, a release of latent heat occurs, providing positive buoyancy. Rosenfeld et al. (2008a) argue that an increase in aerosol number concentration will serve to delay the onset of the collision-coalescence process, and energy is required to lift the parcel containing liquid hydrometeors to lower temperatures. Further increases in the aerosol concentration require the parcel to be lifted to even higher levels before

Aerosol effects on deep convection

J. J. Lebo and
J. H. Seinfeld

Title Page

Abstract

Introduction

Conclusions

References

Tables

Figures

◀

▶

◀

▶

Back

Close

Full Screen / Esc

Printer-friendly Version

Interactive Discussion



collision-coalescence ensues. If collision-coalescence is delayed up to the freezing level, droplets are assumed to freeze, releasing latent heat, and then precipitating from the parcel, removing water mass and generating positive buoyancy. Hydrometeors are assumed to immediately freeze and precipitate if the parcel is lifted even farther. Rosenfeld et al. (2008a) argue that the addition of aerosol particles above that which would occur in a relatively clean environment (i.e., increasing the aerosol number concentration from $\approx 100 \text{ cm}^{-3}$ to $\geq 1000 \text{ cm}^{-3}$) can increase the convective available potential energy (CAPE) of the parcel by $> 1000 \text{ J kg}^{-1}$. The effect of the resultant increase in CAPE and mitigation of the collision-coalescence process is to delay the onset of precipitation, but increase the total precipitation.

The concentration of CCN required to delay collision-coalescence until the parcel reaches the -4°C isotherm is determined from the depth (D) above cloud base needed for precipitation to begin as derived from aircraft measurements (Rosenfeld et al., 2008b; Freud et al., 2008; vanZanten et al., 2005). The result is an aerosol concentration of about 1200 cm^{-3} , assuming standard values for tropical deep convective clouds. Since typical CCN concentrations tend to lie between 100 and 200 cm^{-3} and between 600 and 1700 cm^{-3} in clean and polluted marine regions, respectively (Andreae, 2009), the CCN concentration of 1200 cm^{-3} at which invigoration should reach a maximum is relevant for anthropogenically influenced locations. For concentrations of CCN above 1200 cm^{-3} , collision-coalescence is delayed beyond the freezing level, more energy is required to lift the parcel, and the invigoration effect is mitigated. For higher CCN concentrations, less incoming solar radiation reaches the surface, reducing surface warming, which in turn, stabilizes the boundary layer, hence limiting convective development.

2.2 Stevens and Feingold (2009)

In addition to invigoration of updrafts within and below deep convective clouds, Stevens and Feingold (2009) proposed that an increase in CCN may act to increase cloud top height (i.e., cloud depth). The basis for this hypothesis is that an increase in CCN

Aerosol effects on deep convection

J. J. Lebo and
J. H. Seinfeld

Title Page

Abstract

Introduction

Conclusions

References

Tables

Figures

◀

▶

◀

▶

Back

Close

Full Screen / Esc

Printer-friendly Version

Interactive Discussion



should act both to increase cloud droplet number concentration (N_c) and to reduce cloud droplet effective radius (r_e) in warm clouds, hence delaying the onset of precipitation. This allows hydrometeors to be advected to higher levels, increasing the amount of condensed water within the cloud, in turn increasing evaporation at cloud top, hence cooling and destabilizing the cloud top region. Updrafts near cloud top are invigorated, increasing cloud depth. Since deeper clouds are expected to have more liquid water, an increase in precipitation is expected. However, the microphysical complexity of cold clouds (i.e., those containing ice in some form) adds another dimension, hence the effect of increased aerosols no longer follows such a straightforward pathway.

2.3 Khain et al. (2008)

Khain et al. (2008) attempt to classify the effect of aerosol levels on precipitation from clouds of all types. Using a 2-D CRM with spectral microphysics, Khain et al. (2008) show that deep clouds in both tropical and moist urban areas tend to display an increase in precipitation with increasing aerosol levels. The effect of increased aerosol levels on supercell storms is shown to either decrease or increase precipitation depending upon whether the environment is dry or moist, respectively.

3 Numerical simulation

We explore the effects of aerosol perturbations on deep convective clouds by using the Weather Research and Forecasting (WRF) model Version 3 (Skamarock et al., 2008) as a CRM. The dynamical core of the WRF model is augmented by a detailed mixed-phase bin microphysics scheme following Tzivion et al. (1987), Tzivion et al. (1989), Feingold et al. (1988), Reisin et al. (1996), and Khain et al. (2004). In addition, we provide comparisons between predictions of the detailed bin model and those of a modified two-moment five-class (i.e., cloud, rain, pristine ice, snow, and graupel) bulk microphysics scheme (Morrison et al., 2005; Morrison and Pinto, 2005). The bin

Aerosol effects on deep convection

J. J. Lebo and
J. H. Seinfeld

[Title Page](#)[Abstract](#)[Introduction](#)[Conclusions](#)[References](#)[Tables](#)[Figures](#)[◀](#)[▶](#)[◀](#)[▶](#)[Back](#)[Close](#)[Full Screen / Esc](#)[Printer-friendly Version](#)[Interactive Discussion](#)

scheme and the modifications to the bulk scheme are described in detail below.

3.1 Bin microphysics scheme

The mixed-phase bin microphysics scheme divides each hydrometeor spectrum into 32 bins (i.e., $x_{j_1}, x_{j_2}, \dots, x_{j_{32}}$, where j corresponds to the hydrometeor type: c, i, s, and g for liquid cloud droplets, pristine ice, snow, and graupel, respectively, and x is the mass) with mass doubling between bins such that

$$x_{k+1} = 2x_k \quad (1)$$

in which k corresponds to the lower boundary of bin number k . The mass of the smallest bin is defined to be 1.598×10^{-14} kg (Reisin et al., 1996), which, for liquid droplets (with density $\rho_l = 1000$ kg m⁻³) corresponds to a diameter of 3.125 μ m. Additionally, we assume fixed bulk densities for the frozen species, i.e., $\rho_i = 900$ kg m⁻³, $\rho_s = 200$ kg m⁻³, $\rho_g = 500$ kg m⁻³. The choice of 32 bins allows hydrometeors to attain appreciable sizes for precipitation to occur while minimizing the risk of creating numerical instability due to very large particles falling through grid boxes within a single time step.

3.1.1 Collision-coalescence, accretion, riming, and aggregation

The collision-coalescence process is represented by the moment-conserving numerical solution to the stochastic collection equation of Tzivion et al. (1987) for the first two moments of each distribution, namely the number concentration (N_{j_k}) and mass mixing ratio (M_{j_k}). For collisions amongst liquid droplets, we use the Long (1974) collection kernel. For ice-ice, ice-snow, ice-graupel, snow-graupel, snow-snow, liquid-ice, liquid-snow, liquid-graupel, graupel-graupel collisions we use the gravitational collection kernel.

Collisions among liquid droplets simply produces larger droplets. As a result, the first moment of the size distribution, the mass, is conserved within the liquid category while the zeroth moment, the number concentration, is reduced. Collisions among other

Aerosol effects on deep convection

Z. J. Lebo and
J. H. Seinfeld

Title Page

Abstract

Introduction

Conclusions

References

Tables

Figures

◀

▶

◀

▶

Back

Close

Full Screen / Esc

Printer-friendly Version

Interactive Discussion



particles, e.g., ice-liquid, ice-ice, etc., are not as straightforward because the collisions may lead to the formation of particles in a different category. Hence, the gain and loss terms for each hydrometeor type and category must be determined following the rules defined in Table 1 (Reisin et al., 1996; Khain et al., 2004). Note that m_l , m_s , and m_i correspond to the masses of the liquid, snow, and ice particles involved in a collision.

3.1.2 Vapor condensation/deposition and evaporation/sublimation

Condensation and evaporation of water to and from liquid drops, as well as deposition and sublimation, can depend strongly on the chosen time step and are highly sensitive to small fluctuations in the supersaturation (both with respect to liquid water as well as ice). Tzivion et al. (1989) formulated the condensational forcing (τ) due to a vapor surplus or deficit (Δq_v) as the integral of the surplus/deficit over a timestep (Δt) as

$$\tau = G(P, T) \int_t^{t+\Delta t} \Delta q_v dt \quad (2)$$

in which $G(P, T)$ is a known function of pressure (P) and temperature (T) defined in Pruppacher and Klett (1997) and Seinfeld and Pandis (2006) and Δq_v is defined as

$$\Delta q_v = q_v - q_s \quad (3)$$

where q_s is the saturated water vapor mixing ratio. By utilizing Eq. (2) we can capture the changes in the vapor surplus within a timestep as a result of phase changes, i.e., condensation/evaporation and deposition/sublimation. The full solution to the condensation equation as derived by Tzivion et al. (1989) for linearized distributions within bins is cumbersome and computationally expensive. Therefore, we employ the method of Stevens et al. (1996) in which the mass and number within a given bin are distributed following a top hat distribution. Moreover, we include gas kinetic effects on the growth of the hydrometeors following Clark (1974) and Stevens et al. (1996) in which the mass

Aerosol effects on deep convection

J. Z. Lebo and
J. H. Seinfeld

[Title Page](#)[Abstract](#)[Introduction](#)[Conclusions](#)[References](#)[Tables](#)[Figures](#)[◀](#)[▶](#)[◀](#)[▶](#)[Back](#)[Close](#)[Full Screen / Esc](#)[Printer-friendly Version](#)[Interactive Discussion](#)

growth equation can be expressed as

$$\frac{dm}{dt} = \frac{m^{2/3}}{m^{1/3} + \ell} G(P, T) \Delta q_v \quad (4)$$

in which ℓ represents a length scale for vapor growth defined as

$$\ell = \ell_o \left(\frac{4}{3} \pi \rho_w \right)^{1/3} \quad (5)$$

5 in which ℓ_o is assumed to be $6.4 \mu\text{m}$. There exists an analytic solution to Eq. (4), and this solution is used for the remapping of the bins due to condensation/evaporation and deposition/sublimation.

3.1.3 Cloud droplet activation

The aerosol size distribution is assumed to follow a single-mode lognormal distribution (Seinfeld and Pandis, 2006),

$$n^d(D_p) \equiv \frac{dN}{d \ln D_p} = \frac{N_a}{\sqrt{2\pi} \ln \sigma} \exp \left[-\frac{\ln^2 \left(\frac{D_p}{D_g} \right)}{2 \ln^2 \sigma} \right] \quad (6)$$

where, N_a is the total aerosol number concentration, σ and D_g are the standard deviation and geometric mean diameter, respectively, and D_p is the particle diameter. The number of activated aerosol particles (N_{act}) is computed during each time step by integrating the size distribution over particles with critical supersaturations that are less than the ambient supersaturation,

$$N_{\text{act}} = \int_0^S n^s(s') ds' \quad (7)$$

where S is the ambient supersaturation and $n^s(s')$ is the critical supersaturation distribution. Given the large linear growth rate of very small cloud droplets (since,

Aerosol effects on deep convection

Z. J. Lebo and
J. H. Seinfeld

Title Page

Abstract

Introduction

Conclusions

References

Tables

Figures

◀

▶

◀

▶

Back

Close

Full Screen / Esc

Printer-friendly Version

Interactive Discussion



$dD_c/dt \propto D_c^{-1}$, where D_c is the cloud droplet diameter), we assume that all activated particles enter the first bin of the cloud droplet distribution (i.e., they are assumed to have a diameter of $3.125 \mu\text{m}$).

3.1.4 Freezing and melting

5 Supercooled cloud drops can freeze to form ice crystals via heterogenous (i.e., contact nucleation, immersion freezing, deposition freezing, etc.) and homogeneous freezing. We must turn to previous studies (Bigg, 1953; Fletcher, 1962; Vali, 1975; Cooper, 1986; Meyers et al., 1992) that have shown via various techniques that the ice nuclei (IN) number concentration (and inherently the number of frozen drops) can be
 10 diagnosed by empirically derived using the ambient environmental conditions. The expression derived by Bigg (1953) for the rate of change of frozen drops with time can be used to express the number of frozen drops in a bin during a time step (N_{f_k}) due to both homogeneous freezing of cloud droplets (for $T < -37^\circ\text{C}$) and immersion freezing ($-37^\circ\text{C} < T < -5^\circ\text{C}$) as (Reisin et al., 1996),

$$15 N_{f_k} = N_{c_k}(t) \left(1 - \exp \left[- \frac{\overline{m_{c_k}}}{\rho_l} A' \exp(B'(T_o - T)) \Delta t \right] \right) \quad (8)$$

where $N_{c_k}(t)$ is the number of cloud drops in bin k at the start of the time step, $\overline{m_{c_k}}$ is the average droplet mass in bin k , and A' and B' are constants defined as $10^{-4} \text{cm}^{-3} \text{s}^{-1}$ and 0.66K^{-1} , respectively, from Orville and Kopp (1977). The frozen mass in bin k is simply $N_{f_k} \overline{m_{c_k}}$. Here, we use Eq. (8) only for homogeneous nucleation of ice
 20 crystals. The nucleation of ice crystals due to immersion freezing is caused by IN being immersed within a cloud droplet. These IN become active at various temperatures. Vali (1975) showed that the number of active immersion IN (N_{im}) can be expressed as a function of temperature in degrees Celsius (T_c) by

$$N_{im} = N_{im_0} (0.1 T_c)^Y \quad (9)$$

Aerosol effects on deep convection

Z. J. Lebo and
J. H. Seinfeld

Title Page

Abstract

Introduction

Conclusions

References

Tables

Figures

◀

▶

◀

▶

Back

Close

Full Screen / Esc

Printer-friendly Version

Interactive Discussion



in which it is assumed that $N_{\text{im}_0} = 10^7 \text{ m}^{-3}$ and $\gamma = 4.4$ for convective clouds. Furthermore, for deposition and condensation freezing, we use the formula of Meyers et al. (1992) to relate the number of deposition and condensation IN (N_d) to that of the ambient supersaturation with respect to ice (S_{ice}) as

$$N_d = N_{d_0} \exp[-0.639 + 12.96S_{\text{ice}}] \quad (10)$$

where $N_{d_0} = 10^{-3} \text{ m}^{-3}$. We distribute evenly the number of droplets that freeze due to deposition and contact freezing.

All frozen hydrometeors are assumed to melt over the course of a single timestep when the ambient temperature of the grid box containing such particles is greater than 0°C . Sensitivity simulations with more sophisticated, and hence more computationally expensive, melting routines that attempt to account for heat transfer within the frozen species demonstrated a qualitatively insignificant change in the results presented here.

3.1.5 Sedimentation

All hydrometeors are assumed to sediment at their terminal fall speeds (v_{t_j} , j corresponding to the particle type). As alluded to above, fall speeds for snow and graupel, are computed from the mass-fall speed relationships determined by Locatelli and Hobbs (1974) for aggregates of unrimed side planes and lump graupel, respectively. The terminal fall speed of ice crystals is computed following Heymsfield and Kajikawa (1987). For the purpose of this study, it is assumed that particles in the ice category are pristine crystals in the shape of thin hexagonal plates (type P1a). Terminal velocities are computed by relating the crystal Davies or Best number (X) to the crystal Reynolds number (N_{Re}) by (Heymsfield and Kajikawa, 1987),

$$X = C_d N_{Re}^2 = \frac{2mD_i^2 g}{\rho_i v^2 A} \quad (11)$$

Aerosol effects on deep convection

J. J. Lebo and
J. H. Seinfeld

Title Page

Abstract

Introduction

Conclusions

References

Tables

Figures

◀

▶

◀

▶

Back

Close

Full Screen / Esc

Printer-friendly Version

Interactive Discussion



where m is the crystal mass, D_i is the crystal dimension, g is the acceleration due to gravity, ν is the kinematic viscosity of air, and A is the crystal cross-sectional area normal to the direction of motion. Moreover, we can express N_{Re} as

$$N_{Re} = \frac{v_{t_i} D_i}{\nu}. \quad (12)$$

5 Using the $X-N_{Re}$ parameterization of Heymsfield and Kajikawa (1987), i.e.,

$$N_{Re} = \alpha X^\beta \quad (13)$$

and the definitions of X and N_{Re} , we can write v_{t_i} in terms of the crystal equivalent hexagonal diameter ($D_{i_{eq}}$) as

$$v_{t_i} = \frac{v\alpha}{D_{i_{eq}}} \left[\frac{2mD_{i_{eq}}^2 g}{\rho_i v^2 A} \right]^\beta \quad (14)$$

10 where, for a hexagonal plate,

$$A = \frac{3\sqrt{3}}{2} D_{i_{eq}}^2. \quad (15)$$

Lastly, Heymsfield and Kajikawa (1987) define $D_{i_{eq}}$ to be equivalent to $D_i \sqrt{\gamma}$ where γ is the crystal area ratio (i.e., the ratio of the crystal area to that of a crystal with the same dimensions). We take $\gamma=0.9$.

15 3.2 Bulk microphysical scheme

For the two-moment bulk microphysics scheme, we use that of Morrison et al. (2005) and Morrison and Pinto (2005), included with the WRF model. The scheme has a fixed cloud drop number concentration (N_c), and the freezing process is parameterized following Cooper (1986). These processes are modified as follows.

Aerosol effects on deep convection

Z. J. Lebo and
J. H. Seinfeld

Title Page

Abstract

Introduction

Conclusions

References

Tables

Figures

◀

▶

◀

▶

Back

Close

Full Screen / Esc

Printer-friendly Version

Interactive Discussion



3.2.1 Cloud droplet activation

We have implemented a state-of-the-art activation scheme following Nenes and Seinfeld (2003) and Fountoukis and Nenes (2005). The scheme allows for a sectional representation of the aerosol size distribution. However, to reduce the computational burden required to predict the number of activated aerosol particles, we assume a single-mode lognormal size distribution as given by Eq. (6). The maximum supersaturation (s_{\max}) in a grid cell is estimated by employing the “population splitting” concept of Nenes and Seinfeld (2003) in which the growth of the subsequently formed cloud droplets is split into two categories: (1) those drops that grow significantly beyond their critical size (D_c) and (2) those drops that experience little growth beyond D_c . The number of activated aerosol particles, or, the number of cloud droplets is then computed by integrating Eq. (6) to get,

$$N_{\text{act}} = \int_0^{s_{\max}} n^s(s') ds' = \frac{N_a}{2} \operatorname{erfc} \left[\frac{2 \ln \left(\frac{s_g}{s_{\max}} \right)}{3\sqrt{2} \ln \sigma} \right] \quad (16)$$

where, erfc is the error function complement, and s_g is the geometric mean critical supersaturation for the critical supersaturation distribution,

$$s_g = \sqrt{\frac{4f_1^3 \rho_s M_s}{27i \rho_w M_w D_g^3}}. \quad (17)$$

Here, ρ_s is the density of the solute, respectively, M_w and M_s are the molecular weights of water and the solute, respectively, i is the van't Hoff dissociation factor, and f_1 is defined by,

$$f_1 = \frac{4\sigma_w M_w}{\rho_w} \quad (18)$$

Aerosol effects on deep convection

Z. J. Lebo and
J. H. Seinfeld

Title Page

Abstract

Introduction

Conclusions

References

Tables

Figures

◀

▶

◀

▶

Back

Close

Full Screen / Esc

Printer-friendly Version

Interactive Discussion



in which σ_w is the surface tension of water. Note that the integral form of Eq. (16) resembles Eq. (7) except that in the former, the upper limit of integration is the predicted S_{\max} whereas in the latter it is the ambient supersaturation (s). For details on calculating S_{\max} see Nenes and Seinfeld (2003) and/or Fountoukis and Nenes (2005).

5 3.2.2 Homogeneous and heterogeneous freezing of cloud droplets

Morrison et al. (2005) and Morrison and Pinto (2005) use the parameterization of Cooper (1986) to predict the number of ice nuclei (IN) at a given temperature. Here, we employ the homogeneous and heterogeneous freezing parameterization for a monodisperse IN population of Barahona and Nenes (2008, 2009) to predict the number concentration of ice crystals (N_i). The physical basis of the parameterization comes from an approximate solution to the system of equations that define a parcel of cloudy air undergoing freezing, i.e., changes in supersaturation with respect to ice, ice water mixing ratio, and the subsequent growth of ice crystals after freezing. For more details on the calculations required to compute N_i , see Barahona and Nenes (2009). Given a predicted value of N_i ($N_i(t+\Delta t)$), the actual rate of freezing can be computed as

$$\frac{dN_i}{dt} \Big|_{\text{frz}} = \frac{N_i(t+\Delta t) - N_i(t)}{\Delta t} \iff N_i(t+\Delta t) > N_i(t) \quad (19)$$

while the rate of change of the ice water mixing ratio due to freezing is straightforward once $dN_i/dt|_{\text{frz}}$ has been computed.

20 4 Experimental setup

The WRF model, modified as described in Sect. 3, is initialized with an idealized sounding typical for continental locales conducive to deep convective development (Figs. 1 and 2). Two soundings are used in order to analyze the extent to which an aerosol-induced effect on deep convection is dependent upon the ambient moisture content,

Aerosol effects on deep convection

J. J. Lebo and
J. H. Seinfeld

Title Page

Abstract

Introduction

Conclusions

References

Tables

Figures

◀

▶

◀

▶

Back

Close

Full Screen / Esc

Printer-friendly Version

Interactive Discussion



i.e., the water vapor mixing ratio (q_v) or relative humidity (RH). The ambient RH is permitted to change with height similar to that of Khain and Lynn (2009), except that in the present study, the RH at the surface is 95% in the moist scenarios and the RH for the drier scenarios is simply 5% less than that of the moist cases (hereinafter these scenarios are referred to as the highRH and lowRH simulations, respectively). Therefore, the RH at the surface is 90% for the lowRH simulations. Recently, Fan et al. (2009) showed that aerosol effects may be negligible on deep convective clouds in high shear environments. As a result, we limit the vertical wind shear by utilizing the standard quarter circle shear wind profile derived from Weisman and Klemp (1982) (Fig. 2). Convection is initiated in the domain with a perturbation (bubble) in the potential temperature field of 1.8°C located in the center of the domain in the north-south direction, and offset to the west in the east-west direction. The horizontal and vertical radii of the bubble are 10 km and 2 km, respectively. Khain and Lynn (2009) looked at the dependency of the aerosol induced effects on deep convective clouds using surface relative humidities of 95% and 85% for the moist and dry cases, respectively. We have increased the surface relative humidity in the lowRH cases since the cumulative domain-averaged precipitation in our simulations was insufficient to draw any definitive conclusions at the lower RH owing mostly to the difference in the magnitude of thermal perturbation used to initiate the convection.

It is important to note that unlike previous studies (e.g., Khain and Lynn, 2009), we choose to use a fixed timestep that is consistent for *all* simulations presented. Doing so does, in fact, increase the computation expense of performing such simulations (by nearly a factor of 2), in comparison to using an adaptive timestep method, in which a large fraction of each simulation is performed with a rather large timestep (i.e., at least twice that chosen here for the fixed timestep). However, the additional expense is necessary since the simulated results can differ both quantitatively and qualitatively when switching from a fixed timestep to an adaptive timestep method. In fact, simulations performed on a smaller domain demonstrate that the effect of even a small perturbation in the ambient aerosol concentration (i.e., from 100 to 200 cm^{-3}) can be

Aerosol effects on deep convectionZ. J. Lebo and
J. H. Seinfeld

Title Page

Abstract

Introduction

Conclusions

References

Tables

Figures

◀

▶

◀

▶

Back

Close

Full Screen / Esc

Printer-friendly Version

Interactive Discussion



Aerosol effects on deep convectionZ. J. Lebo and
J. H. Seinfeld

Title Page

Abstract

Introduction

Conclusions

References

Tables

Figures

◀

▶

◀

▶

Back

Close

Full Screen / Esc

Printer-friendly Version

Interactive Discussion



qualitatively different when a fixed timestep is chosen over that where the timestep is allowed to evolve based upon the stability of the model itself. We find that it is necessary to use a fixed timestep to study the effect of aerosol perturbations on the stability of deep convective clouds because if the timestep is allowed to change with the model's stability, and the cloud contained within the polluted environment is in fact more unstable than its clean counterpart, the timestep will be *smaller* for the polluted simulation. Our sensitivity simulations show that the difference in the timestep can be as much as 2 s during the period of time in which convection is strongest. Since sedimentation is computed as simply the mass flux into and out of a grid box multiplied by the timestep itself, the downward flux of condensed water is ultimately dependent upon the timestep. Hence, the cumulative precipitation can be different between simulations with different aerosol number concentrations due to the difference in the timestep chosen by the model. To remove this uncertainty, we have chosen to fix the timestep at 4 s for all cases.

Another potential shortcoming of previous works (e.g., Fan et al., 2009; Khain and Lynn, 2009) is the choice of boundary conditions. Periodic boundary conditions are often used. However, CRM simulations of transient deep convective cells are not consistent with such boundary conditions. In other words, by choosing periodic boundary conditions, the western boundary of the domain is forced by the eastern boundary, which is physically implausible. We employ open boundaries, so that once a cloud, or fraction of a cloud crosses a boundary, it is no longer within the computational domain, and hence does not affect other regions of the domain, or artificially modify the cumulative precipitation.

Many previous studies that have attempted to analyze aerosol-induced effects on deep convective clouds or compare spectral microphysics to bulk microphysics utilized two-dimensional (2-D) models (e.g., Khain et al., 2004, 2008; Khain and Pokrovsky, 2004; Seifert et al., 2006; Phillips et al., 2007). We use a three-dimensional (3-D) domain. The horizontal domain length is 200 km in both the x - and y -direction while the vertical domain extends from the surface to 20 km. This vertical depth allows us

Aerosol effects on deep convectionZ. J. Lebo and
J. H. Seinfeld

Title Page

Abstract

Introduction

Conclusions

References

Tables

Figures

◀

▶

◀

▶

Back

Close

Full Screen / Esc

Printer-friendly Version

Interactive Discussion



to simulate into the lower stratosphere which is important for properly depicting anvil formation near the tropopause. The horizontal grid spacing is set to 1500 m, and there are 60 stretched grid points in the vertical. The vertical grid spacing is less than 150 m at the surface and stretches to 400 m and 1500 m at 10 km above the surface and at the top of the model, respectively. A time step of 4 s is used to ensure numerical stability. The duration of the simulations is 12 h. This duration allows us to capture the point at which the precipitation rate reaches a maximum and then declines to zero. We understand that even at the resolution used in the current work, although higher than that of previous studies, still higher resolution would be beneficial in order to fully capture the three dimensional dynamical feedbacks resulting from changes in the cloud microphysics. However, the hard disk space and computational time required to perform such simulations with the bin microphysics model are beyond the magnitude of our current resources.

To analyze the potential effects of CCN and IN on deep convective clouds we perform a set of three simulations with varying concentrations of CCN and IN. These simulations are defined as: (1) “Clean” – $N_{\text{CCN}}=100 \text{ cm}^{-3}$, (2) “Semi-Polluted” – $N_{\text{CCN}}=200 \text{ cm}^{-3}$, and (3) “Polluted” – $N_{\text{CCN}}=500 \text{ cm}^{-3}$. For the bulk model, it is assumed that $N_{\text{IN}}=10 \ell^{-1}$ for all simulations in which *only* the CCN number concentration is changed. The “Clean” scenario will be used as the base case. To analyze the potential impact of changes in the aerosol loading when the added particles act as good IN, we perform additional simulations at relatively high RH using bulk microphysics, whereby the IN number concentration is elevated to $100 \ell^{-1}$, and using bin microphysics in which we multiply the predicted IN number concentrations for immersion, deposition, and condensation IN by a factor of 2. Regardless of the microphysics scheme employed for the IN sensitivity tests, the CCN number concentration is doubled from the “Clean” case to 200 cm^{-3} . Hereinafter, the cases with increased IN number concentrations are referred to as “IN-Polluted”. The purpose of the “Semi-Polluted” and “IN-Polluted” cases is to show the effect of an increase in aerosol concentration when the particles act only as CCN and when they are CCN and IN, respectively. We realize

Aerosol effects on deep convectionZ. J. Lebo and
J. H. Seinfeld

Title Page

Abstract

Introduction

Conclusions

References

Tables

Figures

◀

▶

◀

▶

Back

Close

Full Screen / Esc

Printer-friendly Version

Interactive Discussion



that there is a slight discrepancy in the manner in which the IN influence is handled in each model. The increase in available IN for the bulk microphysics model is a factor of 10 whereas the increase in activated IN for the bin model is just a factor of 2. Although the factors are not equivalent, the effect on the total number of ice particles ought to be roughly similar since the bulk model accounts for an increase in the *available* IN, allowing us to calculate explicitly the increase in frozen droplets due to an increase in available good IN, whereas the bin model prescribes the increase in frozen droplets to be exactly twice that which would occur given our current parameterizations of nucleation. In other words, although the IN number concentration is elevated by an order of magnitude in the bulk microphysics model, the increase in the number of droplets that freeze ought to be less than this factor since not every droplet will freeze in a given timestep.

The model used in the present study differs from those of previous works, (e.g., Fan et al., 2009; Khain and Lynn, 2009), in that we simulate the evolution of deep convective clouds at a much higher resolution. It is prudent to increase the spatial resolution so as to capture the important dynamical feedbacks that may result from differential heating caused by phase changes. Moreover, one likely underestimates the maximum supersaturation within a grid cell at coarse resolution. In order to predict the cloud drop number concentration, an accurate depiction of the supersaturation is required. We have addressed this issue in the modified bulk scheme using the activation parameterization of Nenes and Seinfeld (2003) and Fountoukis and Nenes (2005). Sensitivity simulations (not shown) exhibit large discrepancies in the bulk cloud water variables, cumulative precipitation, and dynamical feedbacks (i.e., the track of the deep convective cloud) between simulations at low resolution (i.e., $\Delta x = \Delta y \geq 2000$ km) and higher resolutions (i.e., $\Delta x = \Delta y < 2000$ km). Moreover, we have updated the bin microphysics model of Reisin et al. (1996) to include more accurate collection kernels and collection efficiencies for riming processes. Lastly, we have implemented a state-of-the-art activation scheme (Nenes and Seinfeld, 2003; Fountoukis and Nenes, 2005) and homogeneous and heterogeneous freezing parameterization (Barahona and Nenes, 2008,

2009) into the two-moment bulk microphysics scheme of Morrison et al. (2005) and Morrison and Pinto (2005) as a means of comparison with the bin microphysics results. It is important to note that a key difference between in the bulk model employed in Khain and Lynn (2009) and the present study is that the prior used a fixed value for N_c , while here we predict N_c based on relevant physics and ambient environmental conditions.

5 Results: CCN effects on deep convective clouds

We begin with a comparison between bin and bulk simulations of the potential impact on deep convective cloud development and precipitation as a result of increasing the CCN number concentration. It is important to keep in mind that the purpose of this study is not to predict with great precision the amount of precipitation that may result from the given initial environmental conditions, but instead to numerically determine the extent to which the precipitation patterns and magnitude are altered in response to a modified aerosol loading.

5.1 Effect on precipitation and dynamical feedbacks

5.1.1 High relative humidity

The overall effect of a perturbation in the CCN number concentration is to modify the precipitation amounting from a deep convective storm cloud. We quantify the effect as the domain-average cumulative surface precipitation in Fig. 3 (highRH simulations only). First, one notices that there is a large discrepancy between the total precipitation predicted by the bulk scheme and that of the bin model. Rain production, i.e., autoconversion, is much more efficient in the bulk scheme in comparison to the more refined, detailed bin model. As a result, water is transferred from cloud water to rain water faster in the bulk scheme, in which the collection process for liquid droplets is

Aerosol effects on deep convection

Z. J. Lebo and
J. H. Seinfeld

Title Page

Abstract

Introduction

Conclusions

References

Tables

Figures

◀

▶

◀

▶

Back

Close

Full Screen / Esc

Printer-friendly Version

Interactive Discussion



solely dependent upon q_c and N_c . The bin model, on the other hand, is capable of predicting the evolution of the droplet size distribution with much greater accuracy, taking into account the mass mixing ratio and number concentration at specified sizes. Therefore, it is expected that the magnitude of the cumulative precipitation ought to differ between the simulations performed with the bulk microphysics scheme and those with the bin scheme. This is acceptable since the overarching goal of this work is to understand how precipitation is affected by changes in the CCN number concentration and not necessarily to fully explain the differences between simulations performed with bin and bulk microphysics. With that in mind, the total cumulative precipitation predicted by the bulk model appears to be unrealistically high in certain locales. In Fig. 4, cumulative precipitation after 4 h of simulation time is shown for the suite of scenarios described above under high RH conditions. The two biggest differences between the bulk and bin simulations are that the magnitude of the cumulative precipitation near the storm's center is substantially higher for the simulations in which bulk microphysics is employed and the precipitation pattern also differs. The latter is seen by comparing, e.g., Fig. 4a (bulk) and d (bin) in which we find that the simulation run with bulk microphysics predicts a different trajectory for the northern branch of the system. As the cell splits, the northern cell follows a trajectory more towards due east in the bulk simulation while following a path toward the northeast in the bin simulation. The difference in storm trajectory is likely due to dynamical differences between the two systems, i.e., differences in latent heating and the inherent dynamical feedbacks. The latent heating effects will be discussed in more detail below. However, in general, these differences may be a result of using a simplified approach in a high-resolution model. In other words, as one reduces the model resolution, it should be expected that the deviation of q_c and N_c from some mean state should be reduced, such that the extremes (maxima) are not as large. As a result, autoconversion will then be reduced and precipitation will ultimately be reduced. Therefore, in order to accurately predict the total precipitation using a bulk microphysics model, sub-grid scale fluctuations should be considered using methods like that proposed by Morales and Nenes (2010) to calculate precisely

Aerosol effects on deep convectionZ. J. Lebo and
J. H. Seinfeld

Title Page

Abstract

Introduction

Conclusions

References

Tables

Figures

◀

▶

◀

▶

Back

Close

Full Screen / Esc

Printer-friendly Version

Interactive Discussion



sub-grid scale supersaturations.

Figure 3 shows the domain-averaged cumulative precipitation for the highRH simulations. With the discrepancy between the total amount predicted by the bin model in comparison to that of the bulk scheme aside, we focus on the effect of increased CCN number concentrations on precipitation in each model. The overall effect of a doubling of the CCN number concentration (i.e., from 100 to 200 cm⁻³), using the bin microphysics scheme, is to increase precipitation by 11.0% (Table 2). Hence, in contrast to that which was proposed by Rosenfeld et al. (2008a), a large increase in the CCN number concentration is not necessary to increase the precipitation that results from deep convection. In fact, we find that a further increase in CCN number concentration (i.e., from 200 to 500 cm⁻³) causes a reduction in precipitation predicted using the bin microphysics model. Here lies an additional discrepancy between the two microphysics schemes, since the effect of this additional increase in CCN acts to increase the precipitation predicted by the bulk model. This point will be discussed in more detail below.

In order to understand theoretically how an increase CCN number concentration can increase precipitation from deep convection, we turn our attention to the invigoration arguments of Rosenfeld et al. (2008a) and Stevens and Feingold (2009). We can analyze the invigoration that may result from increased aerosol loading using the buoyancy (B) equation (Houze Jr., 1993):

$$B = g \left[\frac{T^*}{T_a} - \frac{p^*}{p_o} + 0.61q_v^* - q_t \right] \quad (20)$$

where T^* is the perturbed temperature from the ambient state (T_a), p^* is the pressure perturbation from the base state (P_o), q_v^* is the deviation in the ambient water vapor mixing ratio from the reference state, and q_t is the total condensed water mass mixing ratio. From Eq. (20), we see that changes in aerosol concentration can be linked to changes in buoyancy, and consequently vertical velocity, since perturbing the CCN number concentration will lead to changes in q_t and T^*/T_a (through latent heating). However, the effects are counteractive, since an increase in CCN number concentration

Aerosol effects on deep convectionZ. J. Lebo and
J. H. Seinfeld

Title Page

Abstract

Introduction

Conclusions

References

Tables

Figures

◀

▶

◀

▶

Back

Close

Full Screen / Esc

Printer-friendly Version

Interactive Discussion



Aerosol effects on deep convectionJ. Z. Lebo and
J. H. Seinfeld

Title Page

Abstract

Introduction

Conclusions

References

Tables

Figures

◀

▶

◀

▶

Back

Close

Full Screen / Esc

Printer-friendly Version

Interactive Discussion



will increase the number of particles that reach the freezing level, freeze, and grow via vapor deposition, thus increasing the latent heating aloft (i.e., increasing buoyancy). But, the increased heating comes in part from an increase in vapor deposition and thus acts to also increase the q_t (decreasing buoyancy). We see then that if the increase in latent heating comes mostly from more cloud droplets freezing, T^*/T_a will increase more so than q_t and the cloud will be invigorated. While, on the other hand, if vapor deposition is a primary source for warming within the mixed-phase and cold regions of the cloud, the contributions to buoyancy can be offset and thus no invigoration (or potentially even a decrease in buoyancy) can theoretically occur.

To understand how the performed simulations represent potential changes in buoyancy we show q_t in Fig. 5, separated into cloud (solid), rain (dashed), and ice (dotted) water contents. This allows us to analyze the effect of increased aerosol loading on rain water simultaneously. From top to bottom, Fig. 5 demonstrates the evolution of the vertical structure of the deep convective cloud in which initially, cloud water is lofted deep into the mixed-phase region, and the ice exists predominantly above 7 km in the bulk simulations and higher yet in the bin simulations. As time progresses, the condensed mass sediments, ice melts to form liquid droplets that act to increase the rain water mixing ratio. As a result, we see that in both the bin and bulk simulations the rain water content is suppressed initially while the cloud water content is enhanced (Fig. 5a and b). This is a direct result of the fact that smaller particles are less likely to collide, hence reducing the amount of cloud water converted to rain drops, and since the droplets are smaller, their terminal fall speeds are reduced and can be lofted higher in the atmosphere. As time progresses, the peak in the vertical distribution of ice water shifts downward, hence increasing the amount of melt water below the freezing water, ultimately leading to an enhancement in the rain water content for an increase in the CCN number concentration from 100 to 200 cm^{-3} , i.e., from the “Clean” to “Semi-Polluted” case (Fig. 5c and f).

In order for the enhancement in rain water to be caused by some dynamical feedback, we turn to Fig. 6, in which the mean vertical velocity (w) within the convective

core, averaged over 4 to 8 h into the simulation, is shown for all highRH simulations. Here, we define the convective core to contain columns within which the mean vertical velocity between 3.3 km and 11 km is at least 1 m s^{-1} . The temporal average of w encapsulates the period of time in which the rain rate is largest. Any significant dynamical enhancement or invigoration should appear from such an average. We see that, regardless of the CCN number concentration, w is more or less fixed for the simulations using the bulk microphysics scheme (Fig. 6). However, the bin results show a clear enhancement in w due to a doubling of the CCN number concentration on the order of 5% to 15% within the cloud itself. In conjunction with the fact that the cloud droplets are smaller, hence more likely to be lofted into the mixed-phase region of the cloud and freeze, thus increasing the rate of vapor deposition, this enhancement in w helps increase q_t (Fig. 5).

To confirm that additional vapor deposition is the root cause for the increase in B and hence, w , we show time- and domain-averaged latent heating rates in Fig. 7 for the suite of simulations performed. The simulations performed with the bulk microphysics scheme (i.e., Fig. 7a) demonstrate that there the change in latent heating due to changes in CCN number concentration is quite small, regardless of the magnitude of the CCN perturbation. From Eq. (20) we would expect that such a small change would result in a negligible change in w assuming that q_t and if q_t were to have increased, the possibility for a decrease in w exists. Since, from Fig. 5, we see that q_t increases when the CCN number concentration is elevated, the result is a negligible change in w or a decrease in w over the 4 to 8 h period of time in the simulations (Fig. 6a). In short, the bulk model suggests limited convective invigoration due to increases in CCN number concentration, but, does exhibit signs of enhanced precipitation at the surface due to increasing the condensed mass within the mixed-phase region of the cloud. On the other hand, the latent heating rate for the simulations performed with the bin microphysics scheme elicit a different result. Here, in Fig. 7b we see that a doubling of the CCN number concentration (solid to dashed curves) results in an increase in the latent heating and, to a lesser extent, cooling. The net result is an increase in the net latent

Aerosol effects on deep convectionZ. J. Lebo and
J. H. Seinfeld

Title Page

Abstract

Introduction

Conclusions

References

Tables

Figures

◀

▶

◀

▶

Back

Close

Full Screen / Esc

Printer-friendly Version

Interactive Discussion



heating rate of about 1 K h^{-1} between 4 and 8 km above the surface and averaged over the period of time in which the precipitation rate attains a maximum (i.e., between 4 and 8 h into the simulations). This increase in heating outweighs the negative effect on buoyancy owing to the increase in condensed water aloft (Fig. 5) and consequently, we find an increase in w (Fig. 6). The increase in w demonstrates that the convective cloud's dynamics are enhanced, resulting in a stronger overturning circulation that persists for a longer amount of time. The ultimate result is that precipitation particles are formed further into the simulation, leading to an increase in rain water content and ultimately an increase in precipitation after approximately 7 h into the simulation.

The following question is then suggested: why does a further increase in CCN number concentration (from the "Semi-Polluted" to "Polluted" case) not elicit a further increase in precipitation in the bin microphysics simulations? And, why is the change in precipitation of a different sign for the bulk and bin microphysics simulations? Tackling the latter first, as noted above, the bulk simulations demonstrate a negligible change in latent heating rates (Fig. 7) and consequently an insignificant change or decrease in w (Fig. 6). Thus, dynamically, the cloud is not invigorated and the resulting increase in precipitation arises from simply a mass balance argument, i.e., what goes up must come down (assuming that the evaporation of cloud/rain water and sublimation of ice/snow/graupel water is small). In other words, the cumulative precipitation increase results from simply adding more condensed water to the system aloft, that ultimately falls to the ground as precipitation. Conversely, we find that the bin model predicts changes to the dynamical nature of the convective system that provide a nonlinear response to an increase in CCN number concentration.

If we focus our attention on the bin microphysics simulations, Fig. 5 portrays an increase in q_i , and consequently q_t , for an increase in the CCN number concentration to 500 cm^{-3} that is over and above that which we find for the increase in CCN to 200 cm^{-3} , especially around hours 5 and 6 into the simulations. Since the cloud droplets are even smaller in the "Polluted" case, even more droplets reach the freezing level at which point they freeze and grow via vapor deposition. This leads to an

Aerosol effects on deep convectionZ. J. Lebo and
J. H. Seinfeld

Title Page

Abstract

Introduction

Conclusions

References

Tables

Figures

◀

▶

◀

▶

Back

Close

Full Screen / Esc

Printer-friendly Version

Interactive Discussion



increase in condensed mass due to an increase in deposition. Figure 7 shows that the latent heating is increased above 7 km for the “Polluted” case in comparison with both the “Clean” and “Semi-Polluted” cases. If all else were equal between the “Polluted” and “Semi-Polluted” cases, we would expect to find a further increase in w and thus more invigoration. However, Fig. 7 demonstrates that the increase in warming is offset by a substantial increase in cooling above 7 km. Since the particles are smaller (the increase in number and mass is not linear), they are more readily evaporated/sublimated. Therefore, the ice particles that act to ultimately increase the precipitation in the “Semi-Polluted” case are instead lofted high into the cloud, at which point they can be advected away from the core (smaller particles have a smaller terminal fall speed and thus can remain aloft for more time) and sublimate as they are detrained from the cloud top/anvil region. As a result, the increase in q_t for the further increase in CCN number concentration moistens the mid- to upper-troposphere rather than increasing precipitation. In other words, as one moves towards a “Polluted” environment, the aerosol-induced effect on deep convection lies in the subtle competition between sedimentation and evaporation/sublimation timescales. Here, the latter is decreased whilst the former is increased (Fig. 8), thus providing even more time for particles to evaporate on their way to the surface, resulting in what appears to be a positive feedback loop.

These results are further corroborated by viewing the cumulative precipitation at the end of the simulations, shown in Fig. 9. Here, we see that the increase in precipitation from the “Clean” to “Semi-Polluted” case comes from both an increase in the intensity of the rainfall at the center of the convective core before splitting and branching off to the east and an increase in the precipitation surrounding the core from stratiform precipitation. A further increase in the CCN number concentration to that of the “Polluted” case shows that the intensity of the rainfall at the core’s center is mitigated. This is a result of too many particles being lofted to the upper levels and remaining small enough such that they are not capable of falling, melting, and reaching the ground as precipitation, as discussed above. Furthermore, we also see that the extent of the lighter, more

Aerosol effects on deep convectionJ. Z. Lebo and
J. H. Seinfeld

Title Page

Abstract

Introduction

Conclusions

References

Tables

Figures

◀

▶

◀

▶

Back

Close

Full Screen / Esc

Printer-friendly Version

Interactive Discussion



stratiform precipitation is greatly reduced, especially, toward the northwest and southern extent of the portrayed region. Following the logic from above, as the particles are lofted and eventually fall in the “Polluted” scenario, they are more susceptible to evaporation/sublimation, and consequently are less likely to reach the surface as precipitation. This is confirmed by the lack of precipitation in large regions of the domain as shown in Fig. 9c in comparison to Fig. 9a.

5.1.2 Low relative humidity

It has been suggested that various environmental parameters, e.g., vertical wind shear (Fan et al., 2009), ambient relative humidity (Khain et al., 2008; Khain and Lynn, 2009), etc., may influence the aerosol-induced effect on deep convection. Here we extend on the work of Khain et al. (2008) and Khain and Lynn (2009) by analyzing the effect on the aerosol-induced invigoration discussed above due to a small change in ambient relative humidity. It was shown previously that a reduction in the RH by 10% throughout the sounding may act to limit any invigoration, or in fact weaken the convective cloud when aerosols are added to the system. However, in Sect. 5.1.1, we demonstrated the need to simulate the system for more than 4 h in order to capture any and all aerosol-induced effects. Here, we have reduced the RH by just 5% (Fig. 1b) to ensure that deep convection forms in all cases, and we permit the simulations to run for 12 h, in order to encapsulate the period of time in which the rain rate attains a maximum.

From Fig. 10, we see that unlike in the highRH cases, precipitation is suppressed in both the bin and bulk lowRH simulations for all aerosol perturbations. In other words, the bin and bulk microphysics schemes are in agreement on the sign of the aerosol-induced effect of aerosols on deep convection for lower relative humidity (note that the magnitude of the effect is *not* the same however; domain-averaged cumulative precipitation and the relative changes due to increased aerosol loading are shown in Table 2). Figure 11 demonstrates that the rain water content (dashed) is initially suppressed, as expected for increased CCN number concentrations. However, as time progresses, unlike in the highRH simulations (Fig. 5) the rain water content is always highest in

Aerosol effects on deep convection

Z. J. Lebo and
J. H. Seinfeld

Title Page

Abstract

Introduction

Conclusions

References

Tables

Figures



Back

Close

Full Screen / Esc

Printer-friendly Version

Interactive Discussion



Aerosol effects on deep convection

J. Z. Lebo and
J. H. Seinfeld

Title Page

Abstract

Introduction

Conclusions

References

Tables

Figures

◀

▶

◀

▶

Back

Close

Full Screen / Esc

Printer-friendly Version

Interactive Discussion

the “Clean” case (black) for the bin microphysics simulations and at most about equal in all cases for the cases run with bulk microphysics. Since the rain water content for the “Semi-Polluted” and “Polluted” scenarios never exceeds that for the “Clean” case, it is physically not possible for the domain-averaged cumulative precipitation for the perturbed cases to exceed that of the “Clean” base case. In comparison to the highRH cases (Fig. 5), we see that the ice water content, on average, increases by a smaller magnitude in the lowRH scenario due to increased aerosol loading. Without an increase a substantial increase in the ice water and a prolonged ice generation process, the cold rain process is limited, hence resulting in less melting and ultimately, no increase in precipitation at the surface.

Following the same line of logic as for the highRH cases, to analyze the dynamical feedback that occurs when the CCN number concentration is perturbed, we show the mean vertical velocity for each polluted scenario and the changes therein due to such perturbations in Fig. 12. Comparing Figs. 6 and 12, we see that there is a consistent increase in w when the ambient moisture profile is reduced to that for the lowRH cases. This is not surprising, since the last two terms in Eq. (20) demonstrate that a decrease in q_v and/or an increase in condensed total water will decrease B . Here, for the lowRH cases, q_v is reduced, but the reduction in condensed water mass, on average, outweighs the change in q_v such that the mean w within the convective core is elevated when the RH is reduced. With that said, it may come as a surprise that w tends to increase as the CCN number concentration increases for simulations performed with both the bin and bulk microphysics schemes under relatively low RH conditions, unlike that for the highRH cases. In fact, the bin simulations show an increase in w of 2 to 10% while the bulk simulations suggest an increase of 8 to 16% throughout most of the vertical profile of the convective core (Fig. 12b). This elicits the question: Why is the cloud “invigorated” but the precipitation is mitigated?

The key to answering this question is to note first that the mean profile of w is for that of the convective core itself. Hence, details of the changes in evaporation, sedimentation, etc., as a result of increasing the CCN number concentration may not be

included in such a figure. Therefore, we show in Fig. 13 the domain-averaged latent heating profiles for the lowRH simulations. To fully understand the effect of reducing the RH on the aerosol-induced effect on deep convection, we compare Figs. 7 and 13. For the bulk simulations under low RH conditions, there is again no significant change in latent heating due to increases in CCN number concentration. However, the latent heating (due mostly to condensation and deposition) is slightly reduced due to lower supersaturations. Hence, the net latent heating profile suggests somewhat less warming overall and even net cooling around 3 km above the surface. Similar to that for the highRH cases, the bin microphysics scheme better predicts changes in latent heating due to changes in aerosol loading for the lowRH simulations. Focusing our attention on the upper level of the cloudy region in Figs. 13b and 7b (i.e., between 8 and 13 km above the surface) we see that although the sign of the change in heating rates for increased CCN number concentration is identical for both RH scenarios, the magnitude is not. In fact, the increase in warming due to an increase in the CCN number concentration is less for the lowRH scenario (less water vapor available to deposit onto condensed cloud particles). While on the other hand, the increase in cooling aloft for an identical increase in CCN number concentration results in more cooling in the lowRH scenario for both the “Semi-Polluted” and “Polluted” cases. In other words, condensation/deposition is slightly reduced but evaporation/sublimation is enhanced for a decrease in RH as one may expect. The warming due to phase changes occurs predominantly within the convective core itself, while the cooling occurs at the cloud boundaries. Therefore, an increase in the warming within the cloud surrounded by an increase in cooling due to an elevated CCN number concentration can and does result in an increase in the overturning circulation of the system and hence an increase in w (Fig. 12). Moreover, it is this increase in evaporation/sublimation aloft (Fig. 13) that ultimately leads to a reduction in the domain averaged precipitation (Fig. 10) for the lowRH cases. As mentioned above for bin simulations for the highRH scenario, there exists a competition between evaporation and sedimentation that ultimately controls the sign of the aerosol-induced effect on the precipitation resulting from deep convection. By

Aerosol effects on deep convectionJ. Z. Lebo and
J. H. Seinfeld

Title Page

Abstract

Introduction

Conclusions

References

Tables

Figures

◀

▶

◀

▶

Back

Close

Full Screen / Esc

Printer-friendly Version

Interactive Discussion



reducing q_v in the lowRH scenario, we essentially reduce the total condensed water mass in the cloud itself. Hence, all else being equal, particles in the “Clean” case will be smaller under the relatively low RH conditions in comparison to that of higher RH. The same goes for the “Semi-Polluted” and “Polluted” cases. As a result, the sedimentation timescale of the particles aloft is increased while the evaporation timescale is reduced for a decrease in RH. As a result, for even the smallest increase in the CCN number concentration shown (i.e., doubling from 100 to 200 cm^{-3}), the evaporative effect outweighs the sedimentation rate and so consequently, less condensed water is converted to rain water and thus less precipitation is observed at the surface. In fact, the increase in evaporation actually further decreases the sedimentation rate of cloud particles. The overall decrease in the mean sedimentation rate of cloud particles due to increased aerosol loading is shown in Fig. 14. Here, we see that there is in fact a nearly monotonic decrease in the sedimentation rate with that of increasing CCN number concentration. For the domain-averaged precipitation to increase, the sedimentation rate would have to increase, especially near the surface, as is the case for the “Semi-Polluted” highRH simulation (Fig. 8).

As demonstrated for the highRH cases in Fig. 9, the effect of increasing the CCN number concentration on the cumulative precipitation is best portrayed as contours of precipitation at the end of the the simulations. Figure 15 shows the cumulative precipitation for the lowRH simulations using the bin microphysics scheme. Comparing Figs. 9 and 15, it is clear that the ambient moisture abundance can and does affect the storm dynamics regardless the aerosol loading. Here, in the lowRH simulations, the northern branch of the storm, after separating from the main core, follows a NNE trajectory, where as the highRH counterparts follow more of a NE trajectory. In regard to the precipitation patterns among the lowRH simulations, one find that the precipitation appears to be more intense in some locales for elevated CCN concentrations (especially for the “Polluted” case in comparison to that of the “Clean” case where more orange, signifying higher precipitation amounts, is observed in the former case; Fig. 15a and c). However, it was shown in Fig. 10 that an increase in the CCN number concentration

Aerosol effects on deep convectionZ. J. Lebo and
J. H. Seinfeld

Title Page

Abstract

Introduction

Conclusions

References

Tables

Figures

◀

▶

◀

▶

Back

Close

Full Screen / Esc

Printer-friendly Version

Interactive Discussion



results in a decrease in the domain averaged cumulative precipitation under relatively low RH conditions. From Fig. 15 it is concluded that the net decrease in precipitation occurs as a result of a less broad swath of precipitation emanating from the original core of the storm. In other words, although the precipitation may be enhanced in some locales (caused by variety of potential effects, e.g., smaller, more numerous particles create an environment more conducive to riming), the domain average is dominated by the breadth of the precipitation swath.

In Sect. 5.1.1 it was shown for the highRH scenario that a slight increase in the CCN number concentration could result in an increase in the domain-averaged cumulative precipitation due to both increases in the localized rainfall intensity and an increase in the area of the region over which significant precipitation falls. On the other hand, when the RH is reduced, localized rainfall rates and overall intensity may increase as well, but the reduction in the saturation ratio dominates the cloud boundaries, resulting in an increase in evaporation/sublimation that ultimately leads to a reduction in the area over which significant measurable precipitation falls. Therefore, regardless of the ambient moisture profile, it is concluded that aerosol-induced changes to the mean precipitation resulting from a deep convective storm are dominated by the areal extent of the region of significant precipitation and not the localized intensity.

5.1.3 Cloud top height effects

To shed light on the potential impact of cloud top height in controlling the amount of precipitation that results for a perturbed deep convective cloud (Stevens and Feingold, 2009), we show the change in cloud top height in Fig. 16 for the “Semi-Polluted” and “Polluted” cases relative to that of the “Clean” case for both microphysical schemes. There is a rather consistent, but small, increase in cloud top height for the simulations performed using the bulk microphysics scheme whereas the opposite is found for those in which the bin scheme is employed. Regardless of sign, the changes are quite small, especially if we restrict ourselves to the period of time before 6 h. The reason for a modest change in the cloud top height, as suggested might occur by Stevens and Feingold

Aerosol effects on deep convection

Z. J. Lebo and
J. H. Seinfeld

Title Page

Abstract

Introduction

Conclusions

References

Tables

Figures

⏪

⏩

◀

▶

Back

Close

Full Screen / Esc

Printer-friendly Version

Interactive Discussion



(2009), is because the clouds in question in this study are very deep, extending from the lifted condensation level (LCL) to the tropopause. Without a significant increase in vertical velocity near the equilibrium level, i.e., just below the tropopause, allowing moisture to punch higher into the lower stratosphere, it is very difficult to increase the height of such a cloud and hence increase the amount of condensed water mass due solely to adiabatic lifting of moist parcels.

6 Results: IN effects on deep convective clouds

An important feature of the models employed in this study, especially the bulk microphysics scheme, is the ability to analyze and evaluate the potential impact of changes in IN number concentration on deep convection. As described in Sect. 3.2, the bulk microphysics scheme used here employs a detailed, physically-based parameterization of ice nucleation that incorporates the ambient IN number concentration (Barahona and Nenes, 2008, 2009). This is important because, as shown previously by Barahona and Nenes (2009) the number of available IN acts to control whether the predominant freezing mechanism is homogeneous or heterogenous. In other words, as the IN number concentration increases, physically the number of droplets that freeze and consequently grow via vapor diffusion should increase at warmer temperatures, thus depleting the ambient vapor surplus and limiting the number of droplets that freeze via homogeneous freezing at much colder temperatures.

Figure 17 demonstrates the effect of an increase in the IN number concentration for both microphysics models in conjunction with an increase in the CCN number concentration. Similar to that which was found for increasing the CCN concentration to the “Polluted” level in the highRH cases, the sign of the resulting influence on the domain-averaged cumulative precipitation from an increase in IN number concentration does not agree for the two microphysics models, i.e., the bulk model suggests that the precipitation will increase further when IN are added to the domain, whereas the bin model demonstrates a significant decrease in the precipitation due to an increase in IN.

Aerosol effects on deep convection

Z. J. Lebo and
J. H. Seinfeld

Title Page

Abstract

Introduction

Conclusions

References

Tables

Figures

◀

▶

◀

▶

Back

Close

Full Screen / Esc

Printer-friendly Version

Interactive Discussion



Table 3 shows the relative change in precipitation as a result of the aforementioned changes in the IN number concentration.

To understand this dichotomy, shown in Fig. 18 are the vertical profiles of condensed water contents for cloud (solid), rain (dashed), and total ice (dotted) water content. As demonstrated above, the increase in precipitation for the simulations using bulk microphysics is corroborated with the increase in rain water content near the surface, especially around hours 6 and 7 into the simulations. Conveniently, this is the time during which the domain-averaged cumulative precipitation for the “IN-Polluted” case exceeds both the “Clean” and “Semi-Polluted” cases. The idea here is that as the number of IN are increased, so does the number of ice particles, i.e., more droplets freeze. Since the equilibrium vapor pressure over a liquid droplet is much higher than that of an ice crystal at temperatures below 0°C, the ice will grow more rapidly. Therefore, the ice water content is increased for the “IN-Polluted” case (Fig. 18). As the particles grow and become more massive, their fall speeds become large enough to allow the particles to fall to the melting level at which point they are converted to rain drops and precipitate out, hence increasing the domain-averaged cumulative precipitation.

Furthermore, from Fig. 18c, at 5 h into the simulations, we see that the cloud water content is higher for the “IN-Polluted” case in comparison to that of the “Semi-Polluted” case, as expected given the above discussion on potential effects of increasing the IN number concentration; more cloud droplets freeze at warmer temperatures, thus limiting the supersaturation aloft and enhancing the supercooled liquid water content. However, if the ice mass and number are enhanced *and* the supercooled liquid droplet mass is as well, riming becomes more efficient and so the supercooled cloud water ultimately gets converted to ice, making the ice crystals even more massive. This conclusion can be observed in Fig. 18g, in which at 7 h into the simulation we see that the ice water content is highest for the “IN-Polluted” case and the supercooled cloud water content is now about equal to that of the other scenarios.

On the other hand, the decrease in the domain-averaged cumulative precipitation for the simulations with bin microphysics is explained following the same line of reasoning

Aerosol effects on deep convectionZ. J. Lebo and
J. H. Seinfeld

Title Page

Abstract

Introduction

Conclusions

References

Tables

Figures

◀

▶

◀

▶

Back

Close

Full Screen / Esc

Printer-friendly Version

Interactive Discussion



as that which was used above for the decrease observed for an increase in the CCN number concentration from the “Semi-Polluted” to “Polluted” case. The bin model, with its physically based spectral resolution, allows for the sedimentation velocities to be more accurately diagnosed, since a prescribed size distribution is not presumed.

Therefore, even though the changes in the bulk condensed water quantities are similar between the bin and bulk results, the particles tend to fall more slowly in the bin microphysics and so the resulting increase in ice water content with the increase in IN does not result in an increase the domain averaged precipitation. We show in Fig. 19 that in fact the mean sedimentation rate of condensed water is suppressed for a doubling in the number of active IN diagnosed in the bin microphysics model compared to both the “Clean” and “Semi-Polluted” cases. We see that the precipitation cannot increase beyond that of the “Semi-Polluted” case because the rain water content is always at most about equal between the two cases. Moreover, the rain water content for the “IN-Polluted” case only exceeds that for the “Clean” case for a brief period of time (i.e., Fig. 18f and h).

Dynamically, the response to an increase in the IN number concentration is consistent with a further increase in the CCN number concentration. In other words, the change in updraft velocity within the convective core for an increase in IN (Fig. 20) is qualitatively similar to that for an increase in the CCN number concentration from the “Semi-Polluted” to “Polluted” case. Specifically, the simulations performed with bulk microphysics again elicit little to no change in latent heating rates for elevated IN number concentrations (Fig. 21a), which results in more or less no change in the vertical velocity within the convective core itself, except near the surface where a slight increase in the cooling rate results in a small net decrease in updraft velocity (Fig. 20b). On the other hand, the simulations performed with bin microphysics demonstrate that if the number of active IN particles is doubled, the latent heating rate increases over that of the “Semi-Polluted” scenario owing to increased depositional growth (as eluded to previously). However, the increases in number and mass are not one-to-one, and so consequently, the particles tend to be small, thus more readily sublimated or evaporated

Aerosol effects on deep convectionZ. J. Lebo and
J. H. Seinfeld

Title Page

Abstract

Introduction

Conclusions

References

Tables

Figures

◀

▶

◀

▶

Back

Close

Full Screen / Esc

Printer-friendly Version

Interactive Discussion



and increase the cooling rate as well (Fig. 21b). The net change in the latent heating rate for the increase in IN number concentration is small, if not somewhat negative. Thus, the mean updraft velocity, especially below 6 km, is suppressed for increase IN concentration. Therefore, it is concluded that small changes in the IN number concentration ought not to cause any significant invigoration in the deep convective cloud.

7 Conclusions

We have presented a high-resolution detailed CRM study (via the WRF model) of the potential effect(s) of aerosol perturbations on the development of deep convective clouds. The study incorporates two different microphysics schemes:

1. Bin Microphysics – a mixed-phase bin microphysics scheme (see Sect. 3.1), based on Tzivion et al. (1987, 1989), Stevens et al. (1996), and Reisin et al. (1996), was coupled to WRF for very detailed microphysics calculations.
2. Modified Bulk Microphysics – the two-moment six-class bulk microphysics scheme of Morrison et al. (2005) and Morrison and Pinto (2005) was modified to include a physically-based parameterization of droplet nucleation (Nenes and Seinfeld, 2003; Fountoukis and Nenes, 2005) and heterogeneous and homogeneous freezing of cloud droplets (Barahona and Nenes, 2008, 2009).

We test the sensitivity of the domain-averaged cumulative precipitation and potential convective invigoration as seen by changes in updraft velocity within the convective core to changes in the ambient aerosol concentration by performing simulations with an increase in the CCN number concentration as well as a suite of cases in which both the CCN and IN number concentrations are increased. The simulated results are compared to the predictions for the base case (i.e., the “Clean” scenario). The dependence of the aerosol-induced effect on the ambient RH is also analyzed.

Under relatively moist ambient conditions, it is shown that a doubling of the CCN number concentration results in an increase in the domain-averaged cumulative

Aerosol effects on deep convection

Z. J. Lebo and
J. H. Seinfeld

Title Page

Abstract

Introduction

Conclusions

References

Tables

Figures



Back

Close

Full Screen / Esc

Printer-friendly Version

Interactive Discussion



precipitation, regardless of the microphysics scheme employed. Increasing the CCN number concentration limits autoconversion and enhances the supercooled liquid water mixing ratio. This leads to an enhancement in freezing and deposition, ultimately leading to an increase in the condensed water mass aloft for an increase in the aerosol loading. The cases run with bulk microphysics suggest little to no invigoration in the updrafts within the convective core, while the bin microphysics scheme, which is shown to better capture changes in latent heating, suggests a slight increase in w within the core itself. However, regardless of the extent to which the cloud is invigorated, the increase in condensed mass ultimately leads to more melting, more rain water, and hence more precipitation. A further increase in the CCN number concentration demonstrates that the aerosol-induced effects may not be monotonic in nature. Simulations performed with the detailed bin microphysics scheme show a decrease in precipitation for the “Polluted” case in comparison with that of the “Clean” case. We propose that the non-monotonic nature of the aerosol effects is the result of a competition between the evaporation/sublimation and sedimentation timescales. The CCN number concentration is increased by a factor of 5 from the “Clean” to the “Polluted” scenario, leading to cloud particles that are significantly smaller in the “Polluted” case. The reduction in particle size acts to increase the sedimentation timescale, while drastically decreasing the evaporation/sublimation timescale. Consequently, under “Polluted” conditions, cloud particles are more likely to evaporate/sublimate before reaching the surface as precipitation leading to a net decrease in the domain-averaged cumulative precipitation. Furthermore, the increase in evaporation/sublimation, in conjunction with an increase in warming due to phase changes within the cloud, acts to invigorate the overturning circulation of the system, driving the updrafts and increasing w . However, this does not necessarily lead to increases in precipitation.

Moreover, when the ambient RH is reduced, an increase in aerosol concentration acts to decrease the domain-averaged cumulative precipitation. As was the case for increasing the CCN number concentration from the “Clean” to “Polluted” scenario under relatively high RH, the competition between evaporation/sublimation and sedimentation

Aerosol effects on deep convectionZ. J. Lebo and
J. H. Seinfeld

Title Page

Abstract

Introduction

Conclusions

References

Tables

Figures

◀

▶

◀

▶

Back

Close

Full Screen / Esc

Printer-friendly Version

Interactive Discussion



dominates the sign of the aerosol-induced effect. Here, under dryer conditions, evaporation/sublimation occurs on even a shorter timescale and as a result dominates the sedimentation for all aerosol perturbations. Thus, a decrease in the rain water content and ultimately precipitation is observed.

5 Changes in the aerosol loading may not necessarily provide particles that act solely as CCN. Some particles are good IN, and thus it is prudent to analyze and understand any and all potential impacts of the IN population on the development of deep convective clouds and the resulting precipitation amount and pattern. The results presented herein suggest that the influence of additional IN is similar in sign, and even in
10 magnitude, to the changes observed for a further increase in the CCN number concentration above the “Semi-Polluted” level. In other words, both microphysics models suggest little to no convective invigoration due to elevated concentrations of IN, but the inherent increase in heterogeneous freezing is observed to ultimately increase the amount of condensed water, mostly in the ice phase. The bulk model, with its pre-
15 defined description for the particle distributions, shows that the increase in mass aloft leads to an increase in precipitation at the surface. While, on the other hand, the simulations performed with bin microphysics, with the ability to predict sedimentation for each segment of the particle distribution, demonstrate that the cloud mass sediments more slowly when the IN concentration is increased (more numerous, smaller particles) in addition to a slight increase in evaporation/sublimation. The end result is that
20 the increased IN number concentration acts to moisten the mid- to upper-troposphere and not to increase the precipitation at the surface.

Our results conclusively demonstrate that any and all changes in the precipitation at the surface are dominated by changes in the mass of condensed water and the competition that exists between evaporation/sublimation and sedimentation and are not related to changes in cloud top height. For shallow convection, Stevens and Feingold (2009) hypothesized that an increase in cloud top evaporation/sublimation due to smaller particles sizes would act to moisten and cool the layer above the cloud and help to deepen the cloud itself. Although we find an increase in evaporation/sublimation
25

Aerosol effects on deep convectionZ. J. Lebo and
J. H. Seinfeld

Title Page

Abstract

Introduction

Conclusions

References

Tables

Figures

◀

▶

◀

▶

Back

Close

Full Screen / Esc

Printer-friendly Version

Interactive Discussion



near the top of the clouds in this study, but the result is not to deepen the clouds since the tops are limited in their height by the tropopause. Thus, any increase in precipitation cannot come from deepening the deep convective cloud, like could be the case for a more shallow convective cloud.

5 An additional important point discussed for all of the sets of simulations performed is that our results demonstrate that the bulk microphysics scheme is not able to capture the domain-averaged changes in latent heating rates due to increased aerosol loading. On the other hand, the bin microphysics model predicts both an increase in warming associated with increases in freezing and deposition aloft, as well as the consequent
10 increase in evaporation/sublimation that results from having more numerous, smaller particles that have a small evaporation/sublimation timescale and a higher sedimentation timescale. Accurately depicting these important details is prudent to fully analyze the potential impacts of changes in the CCN and IN number concentrations on deep convective clouds.

15 Future work to provide a more detailed description of the CCN and IN populations is necessary. Recently, work has been done to relate the number of active IN to the number of CCN particles of considerable size (DeMott et al., 2010). Incorporating this approach into the bin microphysics model would allow one to tie together increases in the CCN and IN number concentrations. Furthermore, a detailed comparison with
20 satellite observed cloud water masses, both liquid and ice, would be beneficial in understanding both how CCN and IN particles can and do modify deep convective clouds. Ideally, an ambient vertical profile of aerosol concentration and type collocated with observations of bulk cloud properties and precipitation is necessary to build upon the current study.

25 *Acknowledgements.* This work was supported by the Office of Naval Research grant N00014-10-1-0200. We thank Thanos Nenes for assistance with incorporating the freezing parameterization into WRF, as well as Jerry Harrington, Adrian Hill, and Graham Feingold for helpful discussions. Computations were carried out on the CITerra Dell Cluster of the Geological and Planetary Sciences Division at Caltech.

Aerosol effects on deep convection

Z. J. Lebo and
J. H. Seinfeld

Title Page

Abstract

Introduction

Conclusions

References

Tables

Figures



Back

Close

Full Screen / Esc

Printer-friendly Version

Interactive Discussion



References

- Ackerman, A. S., Kirkpatrick, M. P., Stevens, D. E., and Toon, O. B.: The impact of humidity above stratiform clouds on indirect aerosol climate forcing, *Nature*, 432, 1014–1017, 2004. 2775
- 5 Albrecht, B.: Aerosols, cloud microphysics, and fractional cloudiness, *Science*, 245, 1227–1230, doi:10.1126/science.245.4923.1227, 1989. 2775
- Andreae, M. O.: Correlation between cloud condensation nuclei concentration and aerosol optical thickness in remote and polluted regions, *Atmos. Chem. Phys.*, 9, 543–556, doi:10.5194/acp-9-543-2009, 2009. 2780
- 10 Barahona, D. and Nenes, A.: Parameterization of cirrus cloud formation in large-scale models: homogeneous nucleation, *J. Geophys. Res.*, 113, D11211, doi:10.1029/2007JD009355, 2008. 2789, 2793, 2806, 2809
- Barahona, D. and Nenes, A.: Parameterizing the competition between homogeneous and heterogeneous freezing in cirrus cloud formation – monodisperse ice nuclei, *Atmos. Chem. Phys.*, 9, 369–381, doi:10.5194/acp-9-369-2009, 2009. 2789, 2794, 2806, 2809
- 15 Bigg, E. K.: The formation of atmospheric ice crystals by the freezing of droplets, *Q. J. Roy. Meteor. Soc.*, 79, 510–519, 1953. 2785
- Clark, T. L.: A study in cloud phase parameterization using the gamma function, *J. Atmos. Sci.*, 31, 142–155, 1974. 2783
- 20 Cooper, W. A.: Ice initiation in natural clouds, *Meteor. Mon.*, 21, 29–32, 1986. 2785, 2787, 2789
- DeMott, P. J., Sassen, K., Poellot, M. R., Baumgardner, D., Rogers, D. C., Brooks, S. D., Prenni, A. J., and Kreidenweis, S. M.: African dust aerosols as atmospheric ice nuclei, *Geophys. Res. Lett.*, 30, 1732–1735, doi:10.1029/2003GL017410, 2003. 2777
- 25 DeMott, P. J., Prenni, A. J., Liu, X., Kreidenweis, S. M., Petters, M. D., Twohy, C. H., Richardson, M. S., Eidhammer, T., and Rogers, D. C.: Predicting global atmospheric ice nuclei distributions and their impacts on climate, *P. Natl. Acad. Sci. USA*, 107, 11217–11222, doi:10.1073/pnas.0910818107, 2010. 2812
- 30 Fan, J., Yuan, T., Comstock, J. M., Ghan, S., Khain, A., Leung, L. R., Li, Z., Martins, V. J., and Ovchinnikov, M.: Dominant role by vertical wind shear in regulating aerosol effects on deep convective clouds, *J. Geophys. Res.*, 114, D22206, doi:10.1029/2009JD012352, 2009. 2776, 2777, 2790, 2791, 2793, 2801

Aerosol effects on deep convection

Z. J. Lebo and
J. H. Seinfeld

Title Page

Abstract

Introduction

Conclusions

References

Tables

Figures

◀

▶

◀

▶

Back

Close

Full Screen / Esc

Printer-friendly Version

Interactive Discussion



Aerosol effects on deep convection

J. Z. Lebo and
J. H. Seinfeld

Title Page

Abstract

Introduction

Conclusions

References

Tables

Figures

◀

▶

◀

▶

Back

Close

Full Screen / Esc

Printer-friendly Version

Interactive Discussion



Feingold, G., Tzivion, S., and Levin, Z.: Evolution of raindrop spectra – Part I: Solution to the stochastic collection/breakup equation using the method of moments, *J. Atmos. Sci.*, 45, 3387–3399, 1988. 2781

Fletcher, N. H.: *The Physics of Rainclouds*, Cambridge University Press, 1962. 2785

5 Fountoukis, C. and Nenes, A.: Continued development of a cloud droplet formation parameterization for global climate models, *J. Geophys. Res.*, 110, D11212, doi:10.1029/2004JD005591, 2005. 2788, 2789, 2793, 2809

Freud, E., Rosenfeld, D., Andreae, M. O., Costa, A. A., and Artaxo, P.: Robust relations between CCN and the vertical evolution of cloud drop size distribution in deep convective clouds, *Atmos. Chem. Phys.*, 8, 1661–1675, doi:10.5194/acp-8-1661-2008, 2008. 2780

10 Heymsfield, A. J. and Kajikawa, M.: An improved approach to calculating terminal velocities of plate-like crystals and graupel, *J. Atmos. Sci.*, 44, 1088–1099, 1987. 2786, 2787

Hill, A. A., Dobbie, S., and Yin, Y.: The impact of aerosols on non-precipitating marine stratocumulus. Model description and prediction of the indirect effect, *Q. J. Roy. Meteor. Soc.*, 134, 1143–1154, doi:10.1002/qj.278, 2008. 2775

15 Hill, A. A., Feingold, G., and Jiang, H.: The influence of entrainment and mixing assumption on aerosol-cloud interactions in marine stratocumulus, *J. Atmos. Sci.*, 66, 1450–1464, 2009. 2775

Houze Jr., R. A.: *Cloud dynamics*, in: *International Geophysics Series*, Vol. 53, Academic Press, Inc., San Diego, California, USA, 1993. 2796

IPCC: Summary for policymakers, in: *Climate Change 2007: The Physical Science Basis, Contribution of Working Group I to the Fourth Assessment Report of the Intergovernmental Panel on Climate Change*, edited by: Solomon, S., Qin, D., Manning, M., Chen, Z., Marquis, M., Averyt, K. B., Tignor, M., and Miller, H. L., Cambridge University Press, 2007. 2775

25 Khain, A. and Lynn, B.: Simulation of a supercell storm in clean and dirty atmosphere using weather research and forecasting model with spectral bin microphysics, *J. Geophys. Res.*, 114, D19209, doi:10.1029/2009JD011827, 2009. 2776, 2778, 2790, 2791, 2793, 2794, 2801, 2822

Khain, A. and Pokrovsky, A.: Simulation of effects of atmospheric aerosols on deep turbulent convective clouds using a spectral microphysics mixed-phase cumulus cloud model – Part II: Sensitivity study, *J. Atmos. Sci.*, 61, 2983–3001, 2004. 2791

30 Khain, A., Pokrovsky, A., Pinsky, M., Seifert, A., and Phillips, V.: Simulation of effects of atmospheric aerosols on deep turbulent convective clouds using a spectral microphysics mixed-

Aerosol effects on deep convectionZ. J. Lebo and
J. H. Seinfeld[Title Page](#)[Abstract](#)[Introduction](#)[Conclusions](#)[References](#)[Tables](#)[Figures](#)[◀](#)[▶](#)[◀](#)[▶](#)[Back](#)[Close](#)[Full Screen / Esc](#)[Printer-friendly Version](#)[Interactive Discussion](#)

phase cumulus cloud model – Part I: Model description and possible applications, *J. Atmos. Sci.*, 161, 2963–2982, 2004. 2778, 2781, 2783, 2791

Khain, A., BenMoshe, N., and Pokrovsky, A.: Factors determining the impact of aerosols on surface precipitation from clouds: an attempt at classification, *J. Atmos. Sci.*, 65, 1721–1748, 2008. 2776, 2778, 2781, 2791, 2801

Koren, I., Kaufman, Y. J., Rosenfeld, D., Remer, L. A., and Rudich, Y.: Aerosol invigoration and restructuring of Atlantic convective clouds, *Geophys. Res. Lett.*, 32, L14828, doi:10.1029/2005GL023187, 2005. 2776

Koren, I., Remer, L. A., Altaratz, O., Martins, J. V., and Davidi, A.: Aerosol-induced changes of convective cloud anvils produce strong climate warming, *Atmos. Chem. Phys.*, 10, 5001–5010, doi:10.5194/acp-10-5001-2010, 2010. 2776, 2777

Locatelli, J. D. and Hobbs, P. V.: Fall speeds and masses of solid precipitation particles, *J. Geophys. Res.*, 79(15), 2185–2197, 1974. 2786

Long, A. B.: Solutions to the droplet collection equation for polynomial kernels, *J. Atmos. Sci.*, 31, 1040–1052, 1974. 2782

Lu, M. and Seinfeld, J. H.: Effect of aerosol number concentration on cloud droplet dispersion: a large-eddy simulation study and implications for aerosol indirect forcing, *J. Geophys. Res.*, 111, D02207, doi:10.1029/2005JD006419, 2006. 2775

Meyers, M. P., DeMott, P. J., and Cotton, W. R.: New primary ice nucleation parameterization in an explicit model, *J. Appl. Meteorol.*, 31, 708–721, 1992. 2778, 2785, 2786

Morales, R. and Nenes, A.: Characteristic updrafts for computing distribution-averaged cloud droplet number and stratocumulus cloud properties, *Geophys. Res. Lett.*, 115, D18220, doi:10.1029/2009JD013233, 2010. 2795

Morrison, H. and Pinto, J. O.: Mesoscale modeling of springtime arctic mixed-phase stratiform clouds using a new two-moment bulk microphysics scheme, *J. Atmos. Sci.*, 62, 3683–3704, 2005. 2781, 2787, 2789, 2794, 2809

Morrison, H., Curry, J. A., and Khvorostyanov, V. I.: A new double-moment microphysics parameterization for application in cloud and climate models – Part I: Description, *J. Atmos. Sci.*, 62, 1665–1677, 2005. 2781, 2787, 2789, 2794, 2809

Nenes, A. and Seinfeld, J. H.: Parameterization of cloud droplet formation in global climate models, *J. Geophys. Res.*, 108(D14), 4415, doi:10.1029/2002JD002911, 2003. 2788, 2789, 2793, 2809

Orville, H. D. and Kopp, F. J.: Numerical simulation of the life history of a hailstorm, *J. Atmos.*

Aerosol effects on deep convectionZ. J. Lebo and
J. H. Seinfeld[Title Page](#)[Abstract](#)[Introduction](#)[Conclusions](#)[References](#)[Tables](#)[Figures](#)[◀](#)[▶](#)[◀](#)[▶](#)[Back](#)[Close](#)[Full Screen / Esc](#)[Printer-friendly Version](#)[Interactive Discussion](#)

Sci., 34, 1596–1618, 1977. 2785

Phillips, V. T. J., Pokrovsky, A., and Khain, A.: The influence of time-dependent melting on the dynamics and precipitation production in maritime and continental storm clouds, *J. Atmos. Sci.*, 64, 338–359, 2007. 2791

5 Pruppacher, H. R. and Klett, J. D.: *Microphysics of Clouds and Precipitation*, Kluwer Academic Publishers, Boston, 1997. 2783

Reisin, T., Levin, Z., and Tzivion, S.: Rain production in convective clouds as simulated in an axisymmetric model with detailed microphysics – Part I: Description of the model, *J. Atmos. Sci.*, 53, 497–519, 1996. 2781, 2782, 2783, 2785, 2793, 2809

10 Rosenfeld, D., Lohmann, U., Raga, G. B., O’Dowd, C. D., Kulmala, M., Fuzzi, S., Reissell, A., and Andreae, M. O.: Flood or drought: how do aerosols affect precipitation?, *Science*, 321, 1309–1313, 2008a. 2776, 2779, 2780, 2796

Rosenfeld, D., Woodley, W. L., Axisa, D., Freud, E., Hudson, J. G., and Givati, A.: Aircraft measurements of the impacts of pollution aerosols on clouds and precipitation over the Sierra Nevada, *J. Geophys. Res.*, 113, D15203, doi:10.1029/2007JD009544, 2008b. 2780

15 Sandu, I., Brenguier, J., Geoffroy, O., Thouron, O., and Masson, V.: Aerosol impacts on the diurnal cycle of marine stratocumulus, *J. Atmos. Sci.*, 65, 2705–2718, 2008. 2775

Sassen, K., DeMott, P. J., Prospero, J. M., and Poellot, M. R.: Saharan dust storms and indirect aerosol effects on clouds: CRYSTAL-FACE results, *Geophys. Res. Lett.*, 30, 1633–1736, doi:10.1029/2003GL017371, 2003. 2777

20 Seifert, A., Khain, A., Pokrovsky, A., and Beheng, K.: A comparison of spectral bin and two-moment bulk mixed-phase cloud microphysics, *Atmos. Res.*, 80, 146–66, 2006. 2791

Seinfeld, J. H. and Pandis, S. N.: *Atmospheric Chemistry and Physics*, 2 edn., John Wiley and Sons, Inc., Hoboken, NJ, 2006. 2783, 2784

25 Skamarock, W. C., Klemp, J. B., Dudhia, J., Gill, D. O., Barker, D. M., Duda, M. G., Huang, X.-Y., Wang, W., and Powers, J. G.: A description of the advanced research WRF Version 3, NCAR Technical Note, National Center for Atmospheric Research (NCAR), Boulder, Colorado, USA, 2008. 2781

30 Stevens, B. and Feingold, G.: Untangling aerosol effects on clouds and precipitation in a buffered system, *Nature*, 461, 607–613, doi:10.1038/nature08281, 2009. 2776, 2780, 2796, 2805, 2811

Stevens, B., Feingold, G., Cotton, W. R., and Walko, R. L.: Elements of the microphysical structure of numerically simulated nonprecipitating stratocumulus, *J. Atmos. Sci.*, 53, 980–

**Aerosol effects on
deep convection**Z. J. Lebo and
J. H. Seinfeld

[Title Page](#)[Abstract](#)[Introduction](#)[Conclusions](#)[References](#)[Tables](#)[Figures](#)[⏪](#)[⏩](#)[◀](#)[▶](#)[Back](#)[Close](#)[Full Screen / Esc](#)[Printer-friendly Version](#)[Interactive Discussion](#)

- 1006, 1996. 2783, 2809
- Teller, A. and Levin, Z.: The effects of aerosols on precipitation and dimensions of subtropical clouds: a sensitivity study using a numerical cloud model, *Atmos. Chem. Phys.*, 6, 67–80, doi:10.5194/acp-6-67-2006, 2006. 2777, 2778
- 5 Twomey, S.: The nuclei of natural cloud formation – Part 2: The supersaturation in natural clouds and the variation of cloud droplet concentration, *Pure Appl. Geophys.*, 43, 243–249, 1959. 2778
- Twomey, S.: The influence of pollution on the shortwave albedo of clouds, *J. Atmos. Sci.*, 34, 1149–1152, 1977. 2775
- 10 Tzivion, S., Feingold, G., and Levin, Z.: An efficient numerical solution to the stochastic collection equation, *J. Atmos. Sci.*, 44, 3139–3149, 1987. 2781, 2782, 2809
- Tzivion, S., Feingold, G., and Levin, Z.: The evolution of raindrop spectra – Part II: Collisional collection/breakup and evaporation in a rainshaft, *J. Atmos. Sci.*, 46, 3312–3327, 1989. 2781, 2783, 2809
- 15 Vali, G.: Remarks on the mechanism of atmospheric ice nucleation, in: *Proceedings of the Eighth International Conference on Nucleation*, St. Petersburg, Russia, 23–29 September, 265–269, 1975. 2785
- Van den Hoever, S. C. and Cotton, W. R.: Urban aerosol impacts on downwind convective storms, *J. Appl. Meteorol. Clim.*, 46, 828–850, 2007. 2776
- 20 Van den Hoever, S. C., Carri, G. G., Cotton, W. R., DeMott, P. J., and Prenni, A. J.: Impacts of nucleating aerosol on florida storms – Part I: Mesoscale simulations, *J. Atmos. Sci.*, 63, 1752–1775, 2006. 2776, 2777
- Wang, H. and Feingold, G.: Modeling mesoscale cellular structures and drizzle in marine stratocumulus – Part I: Impact of drizzle on the formation and evolution of open cells, *J. Atmos. Sci.*, 66, 3237–3256, 2009a. 2775
- 25 Wang, H. and Feingold, G.: Modeling mesoscale cellular structures and drizzle in marine stratocumulus – Part II: The microphysics and dynamics of the boundary region between open and closed cells, *J. Atmos. Sci.*, 66, 3257–3275, 2009b. 2775
- Wang, H., Feingold, G., Wood, R., and Kazil, J.: Modelling microphysical and meteorological controls on precipitation and cloud cellular structures in Southeast Pacific stratocumulus, *Atmos. Chem. Phys.*, 10, 6347–6362, doi:10.5194/acp-10-6347-2010, 2010. 2775
- 30 Weisman, M. L. and Klemp, J. B.: The dependence of numerically simulated convective storms on vertical wind shear and buoyancy, *Mon. Weather Rev.*, 110, 504–520, 1982. 2790, 2823

van Zanten, M. C., Stevens, B., Vali, G., and Lenschow, D. H.: Observations of drizzle in nocturnal marine stratocumulus, *J. Atmos. Sci.*, 62, 88–106, 2005. 2780

Discussion Paper | Discussion Paper | Discussion Paper | Discussion Paper | Discussion Paper

ACPD

11, 2773–2842, 2011

Aerosol effects on deep convection

Z. J. Lebo and
J. H. Seinfeld

Title Page

Abstract

Introduction

Conclusions

References

Tables

Figures

◀

▶

◀

▶

Back

Close

Full Screen / Esc

Printer-friendly Version

Interactive Discussion



Aerosol effects on deep convection

Z. J. Lebo and
J. H. Seinfeld

Table 1. Assumptions regarding hydrometeor collisions.

Collision	Result	Criterion
Liquid-Liquid	Liquid	
Ice-Ice	Snow	
Snow-Snow	Snow	
Graupel-Graupel	Graupel	
Ice-Snow	Snow	
Ice-Graupel	Graupel	
Ice-Liquid	Ice	$m_i \geq m_l$
	Graupel	$m_i < m_l$
Snow-Graupel	Graupel	
Snow-Liquid	Snow	$m_s \geq m_l$
	Graupel	$m_s \geq m_l$
Graupel-Liquid	Graupel	

Title Page

Abstract

Introduction

Conclusions

References

Tables

Figures

◀

▶

◀

▶

Back

Close

Full Screen / Esc

Printer-friendly Version

Interactive Discussion



Aerosol effects on deep convection

Z. J. Lebo and
J. H. Seinfeld

Table 2. Domain-averaged cumulative precipitation at the completion of the simulations performed, $t=12$ h.

Micro.	RH Profile	“Clean” Precip.	“Semi-Polluted” Precip.	Δ Precip. ^a	“Polluted” Precip.	Δ Precip. ^b
Bin	highRH	10.20 mm	11.32 mm	11.0%	7.97 mm	-21.9% (-25.6%)
Bin	lowRH	9.30 mm	8.80 mm	-5.4%	8.09 mm	-13.0% (-8.1%)
Bulk	highRH	45.02 mm	45.61 mm	1.3%	47.50 mm	5.5% (4.1%)
Bulk	lowRH	48.01 mm	42.35 mm	-11.8%	41.86 mm	-12.8% (-1.2%)

^a The relative change in the domain-averaged cumulative precipitation (Δ Precip.) is computed for the “Semi-Polluted” case compared with that of the “Clean” case.

^b Δ Precip. is computed for the “Polluted” case compared with that of the “Clean” case. Δ Precip. between the “Polluted” and “Semi-Polluted” cases is given in parentheses.

[Title Page](#)
[Abstract](#)
[Introduction](#)
[Conclusions](#)
[References](#)
[Tables](#)
[Figures](#)
[Back](#)
[Close](#)
[Full Screen / Esc](#)
[Printer-friendly Version](#)
[Interactive Discussion](#)


Aerosol effects on deep convection

Z. J. Lebo and
J. H. Seinfeld

Table 3. Domain-averaged cumulative precipitation at the completion of the simulations performed including potential IN effects, $t=12$ h.

Micro.	RH Profile	“Clean” Precip.	“Semi-Polluted” Precip.	“IN-Polluted” Precip.	Δ Precip. ^a
Bin	highRH	10.20 mm	11.32 mm	9.10 mm	–19.6% (–10.8%)
Bulk	highRH	45.02 mm	45.61 mm	46.64 mm	2.3% (3.6%)

^a Δ Precip. is computed for the “IN-Polluted” case compared with that of the “Semi-Polluted” case, demonstrating the impact of changes in the IN number concentration. Δ Precip. between the “IN-Polluted” and “Cases” cases is given in parentheses.

[Title Page](#)
[Abstract](#)
[Introduction](#)
[Conclusions](#)
[References](#)
[Tables](#)
[Figures](#)
[Back](#)
[Close](#)
[Full Screen / Esc](#)
[Printer-friendly Version](#)
[Interactive Discussion](#)


Aerosol effects on deep convection

Z. J. Lebo and
J. H. Seinfeld

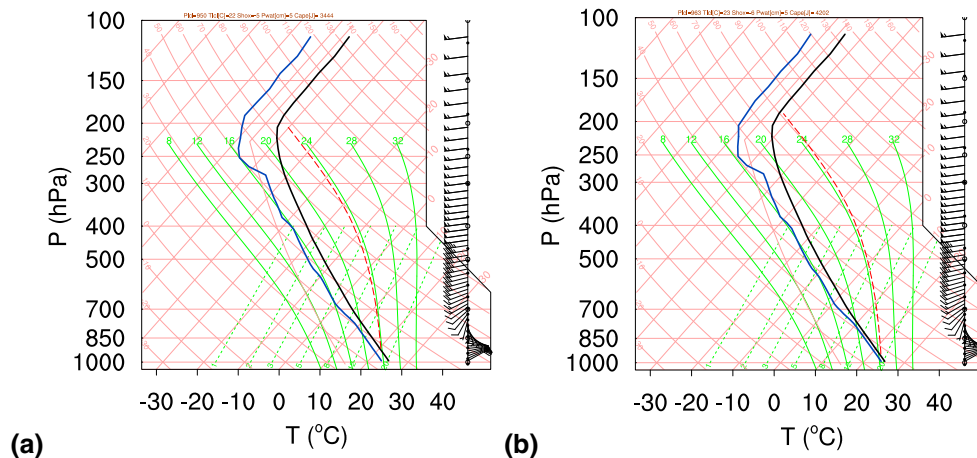


Fig. 1. Skew T -Log- P diagrams of the initial temperature and moisture data for the **(a)** lowRH and **(b)** highRH simulations. The soundings are adopted from Khain and Lynn (2009) with modifications.

Title Page

Abstract

Introduction

Conclusions

References

Tables

Figures

◀

▶

◀

▶

Back

Close

Full Screen / Esc

Printer-friendly Version

Interactive Discussion



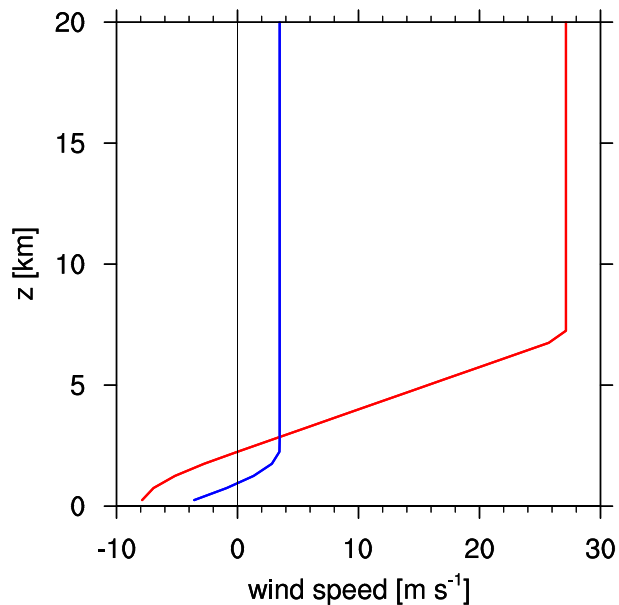


Fig. 2. Quarter circle shear wind profile. The zonal wind (u) is in red and the meridional wind (v) is in blue. The values are derived following Weisman and Klemp (1982) as modified for inclusion in WRF.

Aerosol effects on deep convection

Z. J. Lebo and
J. H. Seinfeld

Title Page

Abstract

Introduction

Conclusions

References

Tables

Figures

◀

▶

◀

▶

Back

Close

Full Screen / Esc

Printer-friendly Version

Interactive Discussion



Aerosol effects on deep convectionZ. J. Lebo and
J. H. Seinfeld

Title Page

Abstract

Introduction

Conclusions

References

Tables

Figures

◀

▶

◀

▶

Back

Close

Full Screen / Esc

Printer-friendly Version

Interactive Discussion

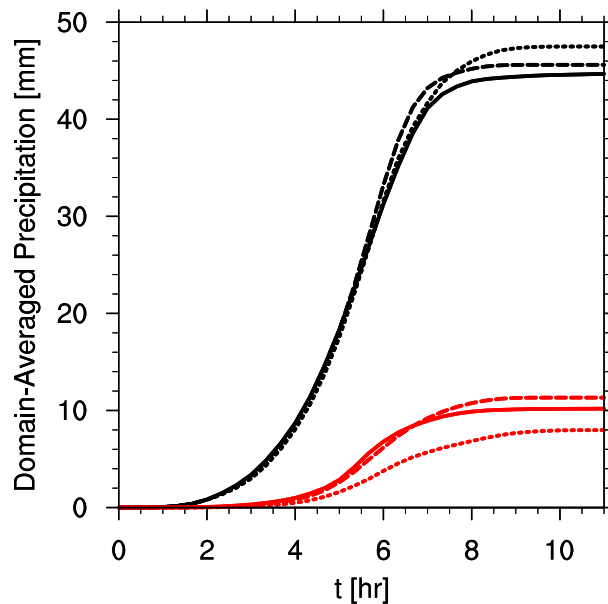


Fig. 3. Domain-averaged cumulative precipitation for the highRH simulations using the bulk (black) and bin (red) microphysics models. CCN effects are shown for the “Clean” (solid), “Semi-Polluted” (dashed), and “Polluted” (dotted) scenarios.

Aerosol effects on deep convection

Z. J. Lebo and
J. H. Seinfeld

Title Page

Abstract

Introduction

Conclusions

References

Tables

Figures

◀

▶

◀

▶

Back

Close

Full Screen / Esc

Printer-friendly Version

Interactive Discussion

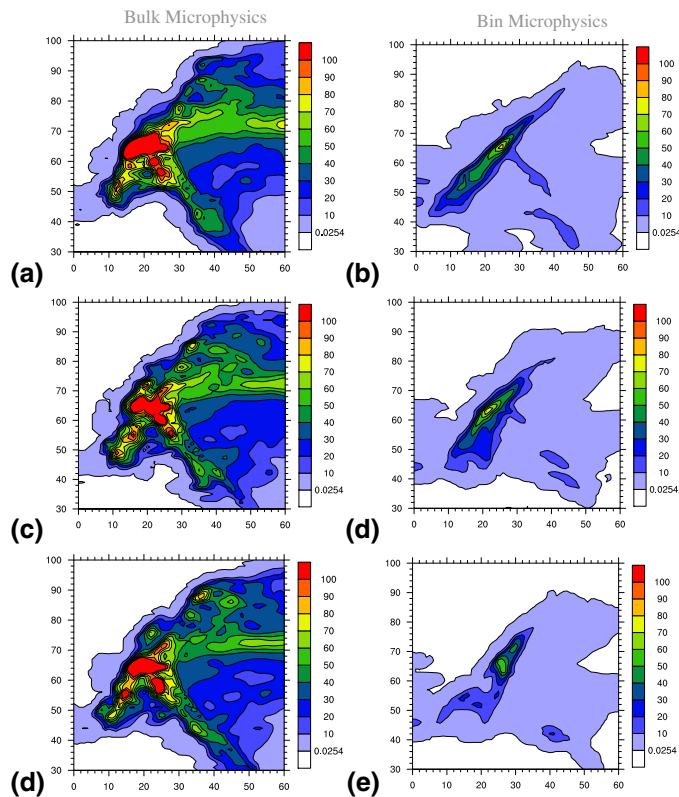


Fig. 4. Cumulative precipitation after 4 h of simulation time for the (a and d) “Clean”, (b and e) “Semi-Polluted”, and (c and f) “Polluted” scenarios for high RH. Simulations performed with bulk microphysics are shown in (a–c) and those with bin microphysics in (d–f). Note that the x - and y -axes represent the grid location index and that the portrayed region is a subset of the entire domain, chosen to elicit the largest differences amongst the set of simulations performed. The first contour level is chosen to be 0.0254 mm, which corresponds to 0.01 in. Any rainfall below this amount is considered to be a trace amount. Consequently, areas shown in white represent regions in which a trace or less of precipitation as fallen.

Aerosol effects on deep convection

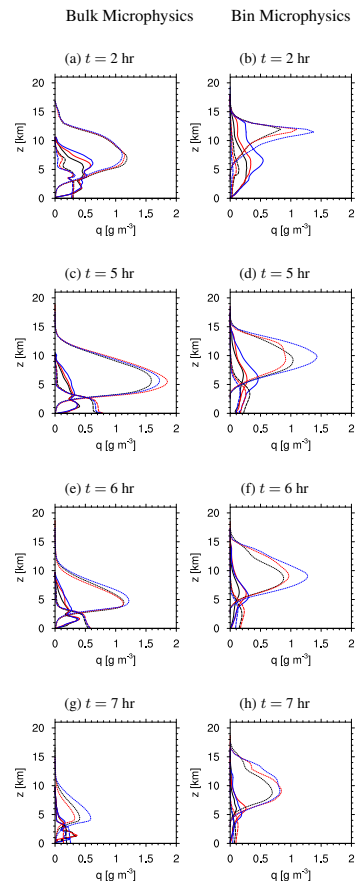
Z. J. Lebo and
J. H. Seinfeld

Fig. 5. Hourly conditionally-averaged cloud (solid), rain (dashed), and ice (dotted) water contents for the bulk (left) and bin (right) simulations. The aerosol sensitivity is shown for the “Clean” (black), “Semi-Polluted” (red), and “Polluted” (blue) scenarios. Simulation time is shown in the subcaptions.

Title Page

Abstract

Introduction

Conclusions

References

Tables

Figures

◀

▶

◀

▶

Back

Close

Full Screen / Esc

Printer-friendly Version

Interactive Discussion



Aerosol effects on deep convection

Z. J. Lebo and
J. H. Seinfeld

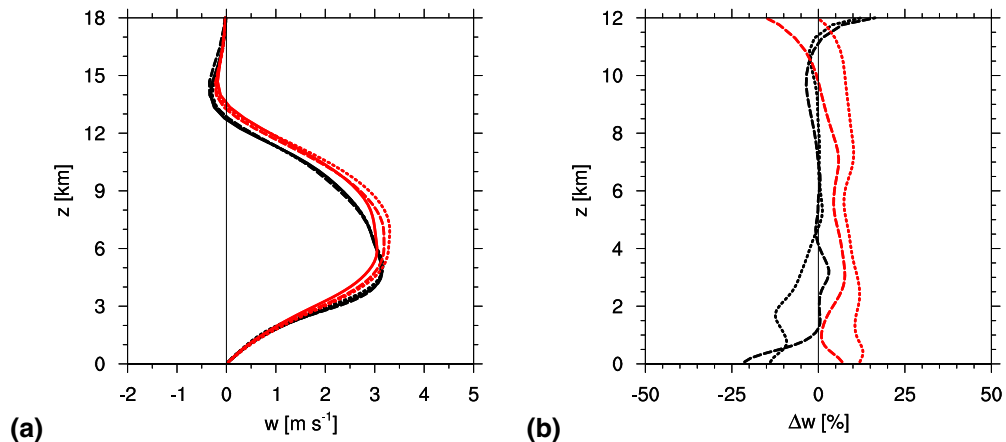


Fig. 6. (a) Temporal average of the vertical velocity profile within the convective core and (b) the change in the mean vertical velocity due to changes in CCN number concentration. The averages are performed from 4 to 8 h into the simulations and the convective core is defined to contain the columns in which the mean vertical velocity is more than 1 m s^{-1} . Bulk (black) and bin (red) are displayed on the same graph. The differences are performed for the “Semi-Polluted” (dashed) and “Polluted” (dotted) cases relative to the “Clean” (solid) case. The vertical axis is different so as to highlight the differences within the cloud itself and because the relative differences at cloud top and above are much larger than those within the cloud.

Title Page

Abstract

Introduction

Conclusions

References

Tables

Figures

◀

▶

◀

▶

Back

Close

Full Screen / Esc

Printer-friendly Version

Interactive Discussion



Aerosol effects on deep convection

Z. J. Lebo and
J. H. Seinfeld

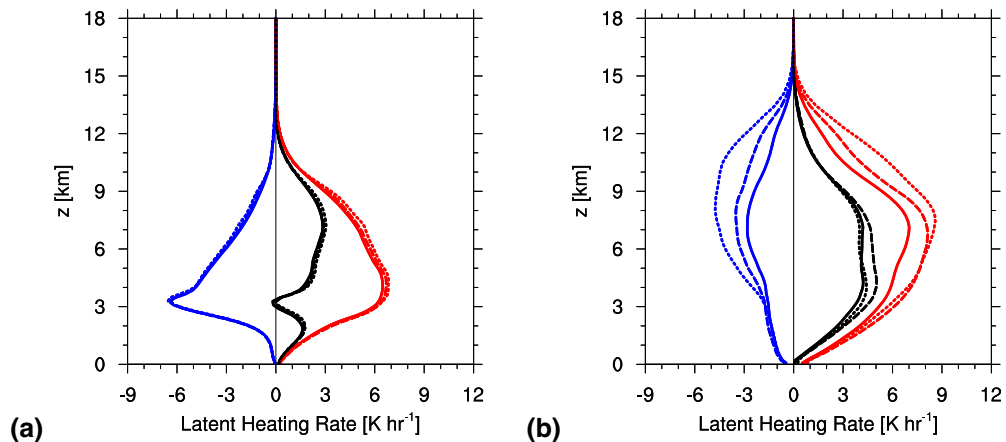


Fig. 7. Domain-averaged latent heating rates for the **(a)** bulk and **(b)** bin microphysics schemes averaged over the same period of time as in Fig. 6. The net heating rate (black) is separated into warming (red) and cooling (blue) for the “Clean” (solid), “Semi-Polluted” (dashed), and “Polluted” (dotted) cases.

[Title Page](#)
[Abstract](#)
[Introduction](#)
[Conclusions](#)
[References](#)
[Tables](#)
[Figures](#)
[◀](#)
[▶](#)
[◀](#)
[▶](#)
[Back](#)
[Close](#)
[Full Screen / Esc](#)
[Printer-friendly Version](#)
[Interactive Discussion](#)

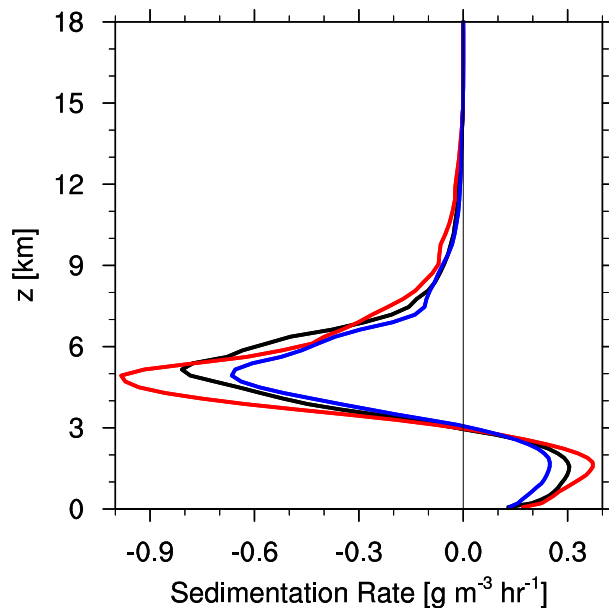



Fig. 8. Domain-averaged sedimentation rate of the total condensed water content for the “Clean” (black), “Semi-Polluted” (red), and “Polluted” (blue) cases using the bin microphysics scheme. The average is computed from 4 to 8 h into the simulations.

Aerosol effects on deep convection

Z. J. Lebo and
J. H. Seinfeld

Title Page

Abstract

Introduction

Conclusions

References

Tables

Figures

◀

▶

◀

▶

Back

Close

Full Screen / Esc

Printer-friendly Version

Interactive Discussion



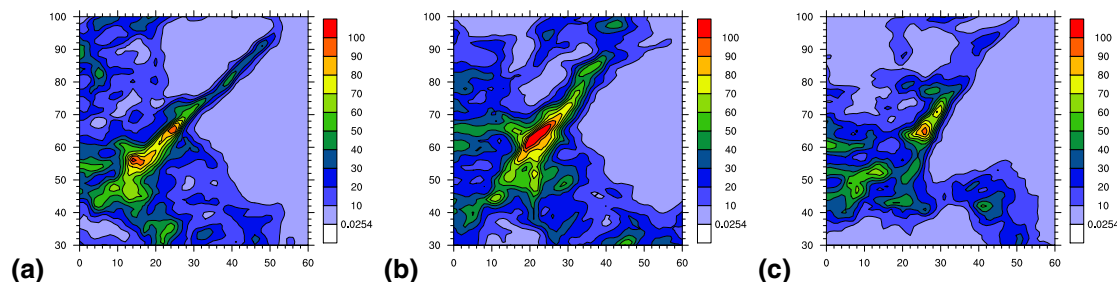
**Aerosol effects on
deep convection**Z. J. Lebo and
J. H. Seinfeld

Fig. 9. Cumulative precipitation after 12h of simulation time for the (a) “Clean”, (b) “Semi-Polluted”, and (c) “Polluted” scenarios for high RH using bin microphysics. The x - and y -axes correspond to location indices and only a subset of the entire domain is chosen to clearly demonstrate differences that arise between simulations.

Title Page

Abstract

Introduction

Conclusions

References

Tables

Figures

◀

▶

◀

▶

Back

Close

Full Screen / Esc

Printer-friendly Version

Interactive Discussion



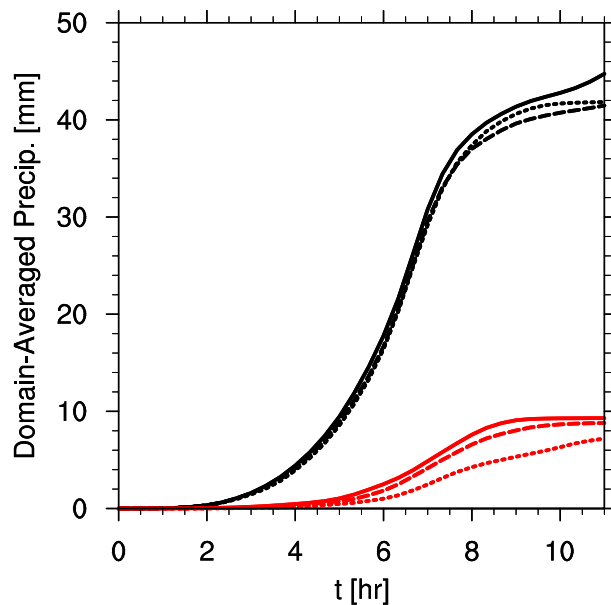


Fig. 10. Same as in Fig. 3 except for the lowRH simulations.

Aerosol effects on deep convection

Z. J. Lebo and
J. H. Seinfeld

Title Page

Abstract Introduction

Conclusions References

Tables Figures

◀ ▶

◀ ▶

Back Close

Full Screen / Esc

Printer-friendly Version

Interactive Discussion



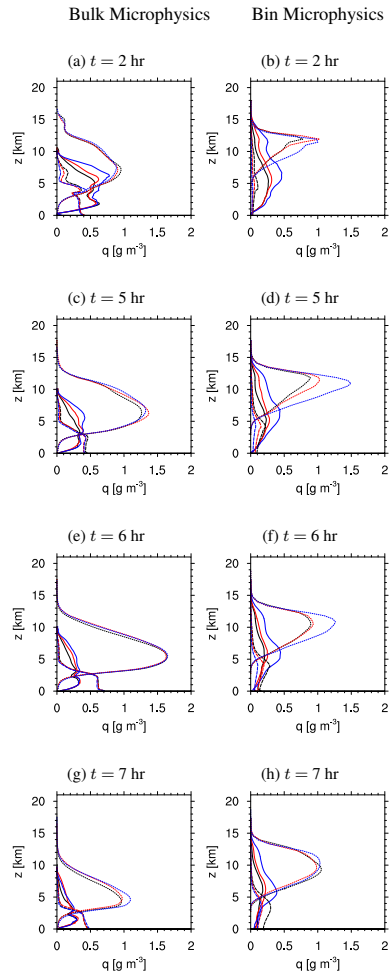


Fig. 11. Same as Fig. 5 except for the lowRH simulations. Simulation time is shown in the subcaptions.

Aerosol effects on deep convection

Z. J. Lebo and
J. H. Seinfeld

Title Page

Abstract

Introduction

Conclusions

References

Tables

Figures

◀

▶

◀

▶

Back

Close

Full Screen / Esc

Printer-friendly Version

Interactive Discussion



Aerosol effects on deep convectionZ. J. Lebo and
J. H. Seinfeld

Title Page

Abstract

Introduction

Conclusions

References

Tables

Figures

◀

▶

◀

▶

Back

Close

Full Screen / Esc

Printer-friendly Version

Interactive Discussion

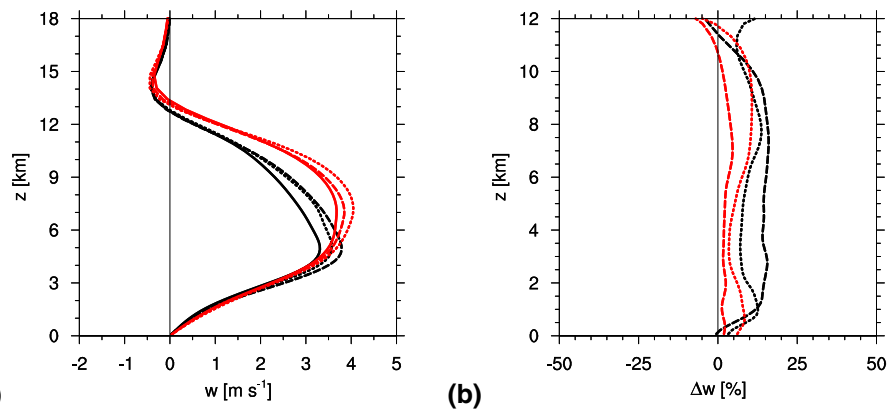


Fig. 12. Same as in Fig. 6 except for the lowRH simulations.

Aerosol effects on deep convectionZ. J. Lebo and
J. H. Seinfeld

Title Page

Abstract

Introduction

Conclusions

References

Tables

Figures

◀

▶

◀

▶

Back

Close

Full Screen / Esc

Printer-friendly Version

Interactive Discussion

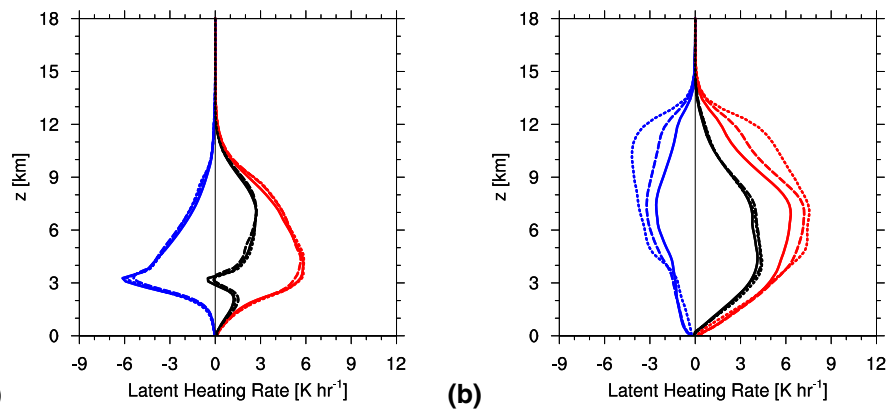


Fig. 13. Same as in Fig. 7 except for the lowRH simulations.

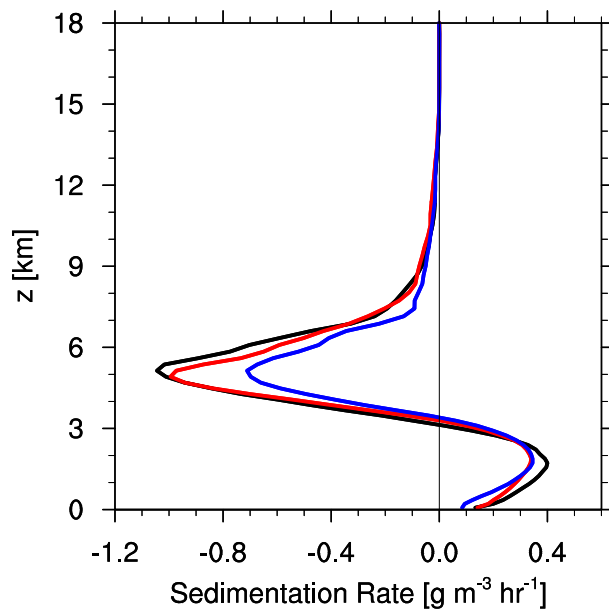


Fig. 14. Same as Fig. 8 except for the lowRH simulations.

Aerosol effects on deep convection

Z. J. Lebo and
J. H. Seinfeld

Title Page

Abstract

Introduction

Conclusions

References

Tables

Figures

◀

▶

◀

▶

Back

Close

Full Screen / Esc

Printer-friendly Version

Interactive Discussion



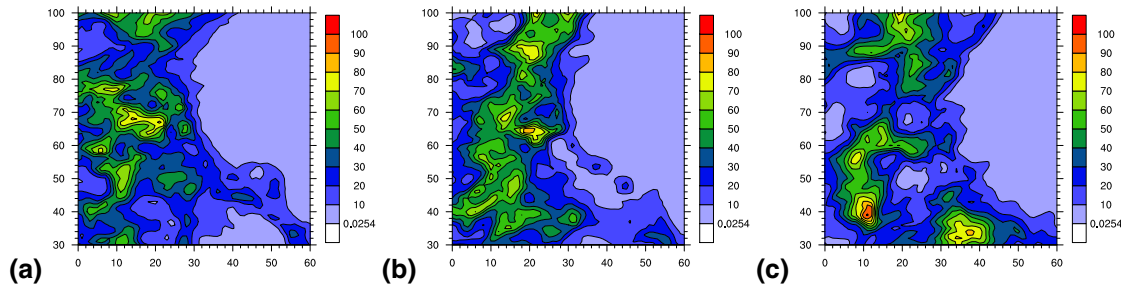
Aerosol effects on deep convectionZ. J. Lebo and
J. H. Seinfeld

Fig. 15. Same as Fig. 9 except for the lowRH simulations performed with bin microphysics.

Title Page

Abstract

Introduction

Conclusions

References

Tables

Figures

◀

▶

◀

▶

Back

Close

Full Screen / Esc

Printer-friendly Version

Interactive Discussion



Aerosol effects on deep convectionZ. J. Lebo and
J. H. Seinfeld

Title Page

Abstract

Introduction

Conclusions

References

Tables

Figures

◀

▶

◀

▶

Back

Close

Full Screen / Esc

Printer-friendly Version

Interactive Discussion

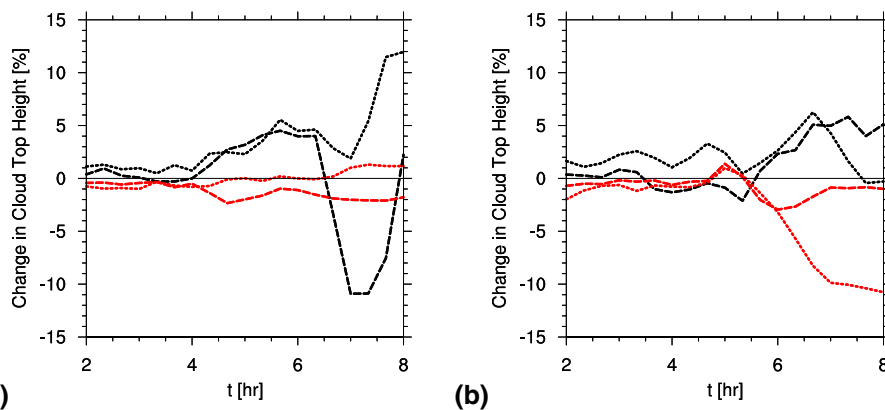


Fig. 16. The change in mean cloud top height is depicted for the “Semi-Polluted” (dashed) and “Polluted” (dotted) scenarios relative to the “Clean” case using both the bulk (black) and bin (red) microphysics schemes. The x-axis is restricted to the middle of the simulation in order to clearly demonstrate any changes in cloud top height during the period of time that convection is enhanced, if at all.

Aerosol effects on deep convectionZ. J. Lebo and
J. H. Seinfeld

Title Page

Abstract

Introduction

Conclusions

References

Tables

Figures

◀

▶

◀

▶

Back

Close

Full Screen / Esc

Printer-friendly Version

Interactive Discussion

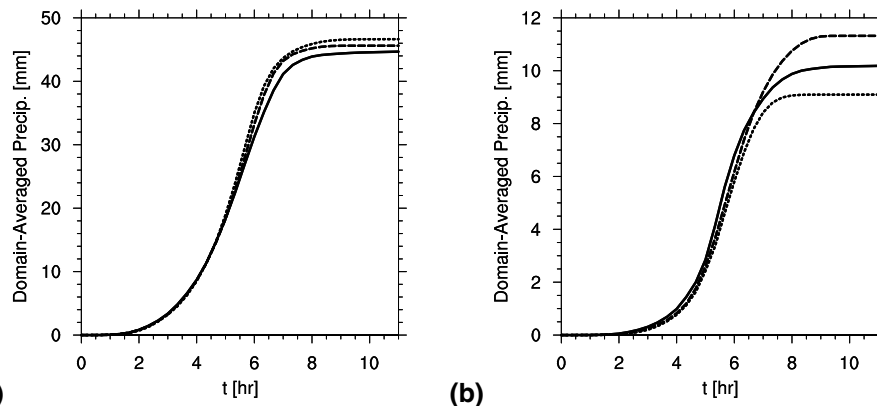


Fig. 17. Domain-averaged cumulative precipitation for the highRH simulations using **(a)** bulk and **(b)** bin microphysics. CCN/IN effects are shown for the “Clean” (solid), “Semi-Polluted” (dashed), and “IN-Polluted” (dotted) scenarios. Note the difference in the y-axis scale between **(a)** and **(b)**. The bulk and bin results have been separated here for clarity.

Aerosol effects on deep convection

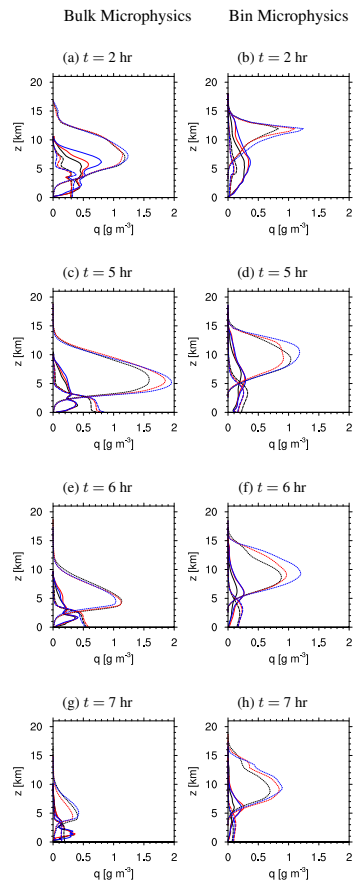
Z. J. Lebo and
J. H. Seinfeld

Fig. 18. Hourly conditionally-averaged cloud (solid), rain (dashed), and ice (dotted) water contents for the bulk (left) and bin (right) simulations. The aerosol sensitivity is shown for the “Clean” (black), “Semi-Polluted” (red), and “IN-Polluted” (blue) scenarios. Simulation time is shown in the subcaptions.

Title Page

Abstract

Introduction

Conclusions

References

Tables

Figures

◀

▶

◀

▶

Back

Close

Full Screen / Esc

Printer-friendly Version

Interactive Discussion



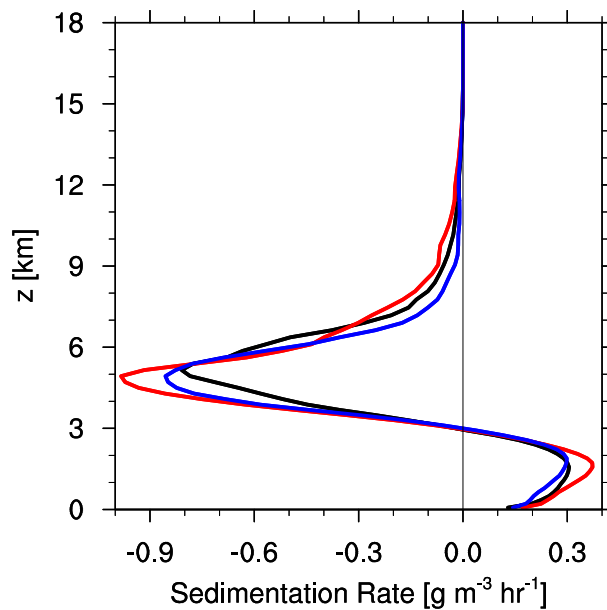
Aerosol effects on deep convectionZ. J. Lebo and
J. H. Seinfeld

Fig. 19. Same as in Fig. 8 except that the “Clean” (solid), “Semi-Polluted”, and “IN-Polluted” cases are shown using bin microphysics.

[Title Page](#)[Abstract](#)[Introduction](#)[Conclusions](#)[References](#)[Tables](#)[Figures](#)[◀](#)[▶](#)[◀](#)[▶](#)[Back](#)[Close](#)[Full Screen / Esc](#)[Printer-friendly Version](#)[Interactive Discussion](#)

Aerosol effects on deep convectionZ. J. Lebo and
J. H. Seinfeld

Title Page

Abstract

Introduction

Conclusions

References

Tables

Figures

◀

▶

◀

▶

Back

Close

Full Screen / Esc

Printer-friendly Version

Interactive Discussion

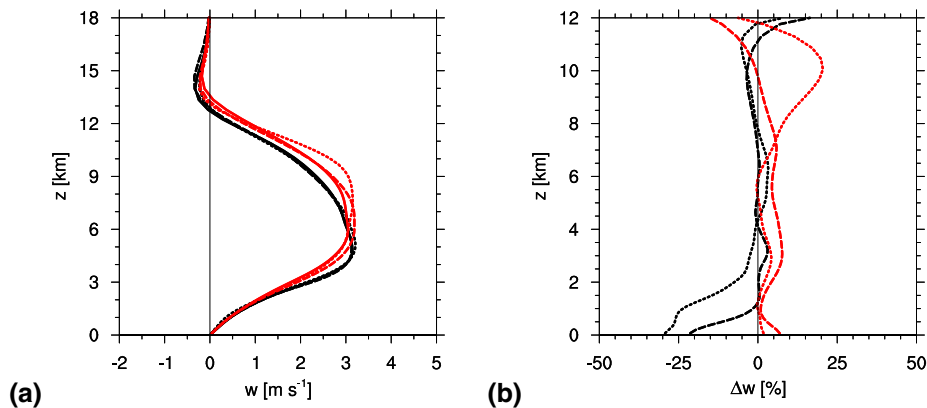


Fig. 20. Same as in Fig. 6 except that the “Clean” (solid), “Semi-Polluted” (dashed), and “IN-Polluted” (dotted) cases are shown.

Aerosol effects on deep convectionZ. J. Lebo and
J. H. Seinfeld

Title Page

Abstract

Introduction

Conclusions

References

Tables

Figures

◀

▶

◀

▶

Back

Close

Full Screen / Esc

Printer-friendly Version

Interactive Discussion

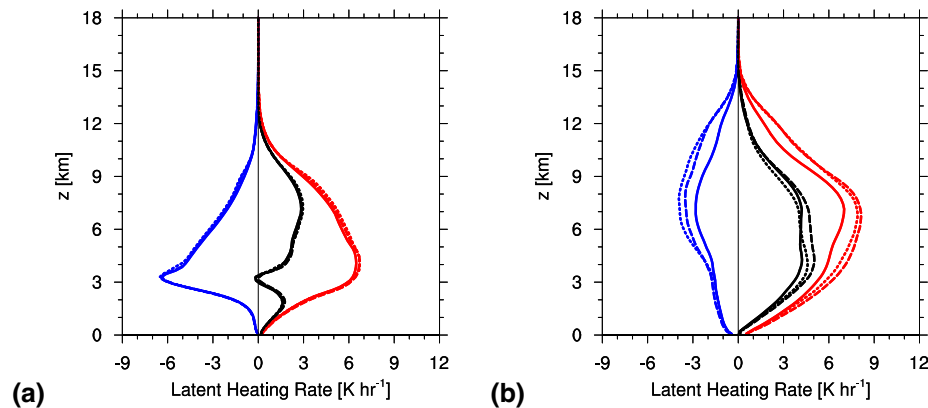


Fig. 21. Same as in Fig. 7 except that the “Clean” (solid), “Semi-Polluted” (dashed), and “IN-Polluted” (dotted) cases are shown.